


# Monitoring the response of Severn Suspension Bridge in the United Kingdom using multi-GNSS measurements

Hussein Alwan Msaewe<sup>1</sup> | Panos A. Psimoulis<sup>2</sup>  | Craig M. Hancock<sup>3</sup> |  
Gethin Wyn Roberts<sup>4,5</sup> | Lukasz Bonenberg<sup>6</sup>

<sup>1</sup>Department of Surveying, College of Engineering, University of Baghdad, Baghdad, Iraq

<sup>2</sup>Nottingham Geospatial Institute, The University of Nottingham, Nottingham, UK

<sup>3</sup>School of Architecture, Building and Civil Engineering, Loughborough University, Loughborough, UK

<sup>4</sup>Department of Land and Sea Mapping, Faroese Environment Agency, Torshavn, Faroe Islands

<sup>5</sup>Faculty of Science and Technology, University of the Faroe Islands, Tórshavn, Faroe Islands

<sup>6</sup>Joint Research Centre (JRC), European Commission, Ispra, Italy

## Correspondence

Panos A. Psimoulis, Nottingham Geospatial Institute, The University of Nottingham, Nottingham, UK.  
Email: panagiotis.psimoulis@nottingham.ac.uk

## Funding information

Ningbo Nottingham New Material Institute, Grant/Award Number: A0060; Ningbo Science and Technology Bureau, Grant/Award Number: 2019C50017

## Summary

The application of GPS in bridge monitoring aims to determine accurately and precisely the response of the deck and towers of the bridge and estimate the main response characteristics (amplitude and modal frequencies). The main requirement of GPS monitoring is a high level of accuracy and availability of fixed solutions, which ensure the reliable operation of GPS and result in the precise estimation of the bridge's response. However, the derived GPS time series of bridge monitoring can be contaminated by noise, due to the performance of the GPS satellite(s), the geometry of the GPS satellite constellation and the potential obstructions due to the bridge elements, which can even lead to GPS solution of poor accuracy and/or precision and result in reduced efficiency of the performance of the GPS monitoring. This study investigates the potential contribution of other Global Navigation Satellite Systems (GNSS) constellations for a more robust and reliable displacement time series solution, derived from multi-GNSS records. More specifically, a novel method is developed to derive the optimal combination of GNSS records to determine the GNSS displacement time series based on checks of parameters which reflect the geometry of the satellite constellation and the quality of the GNSS satellites signals. The method is applied in monitoring of the Severn Suspension Bridge, in the United Kingdom, and it is revealed the enhancement in the GNSS monitoring performance of the bridge response for specific time intervals for various locations on the bridge's support towers, suspension cables and deck.

## KEYWORDS

bridge response, monitoring, multi-GNSS time series, Severn Suspension Bridge, spectral analysis

## 1 | INTRODUCTION

Long-span bridges are one of the key assets of infrastructure, which require continuous structural health monitoring (SHM) in order to evaluate the bridge response, identify potential malfunction and enhance the maintenance of the

-----  
This is an open access article under the terms of the Creative Commons Attribution License, which permits use, distribution and reproduction in any medium, provided the original work is properly cited.

© 2021 The Authors. Structural Control and Health Monitoring published by John Wiley & Sons Ltd.

bridge.<sup>1</sup> The specific design of each long-span bridge and the various external dynamic loadings (i.e., wind, temperature and traffic) result in their complex response. This led to the development of multisensor monitoring systems for long-span bridges; the wind and structural health monitoring system (WASHMS) of Tsing Ma Bridge is a representative example, as it consists of more than 800 sensors.<sup>1</sup> Apart from the traditional monitoring sensors (e.g., accelerometers and strain gauges), the Global Positioning System (GPS) has been introduced in bridge monitoring providing direct 3D displacement, in an independent coordinate system<sup>2,3</sup> and high-sampling rate (up to 100 Hz<sup>3–5</sup>). Several experimental studies have shown that GPS measurements can accurately monitor dynamic motion of a few mm amplitude, that is, 4–5 mm,<sup>6–8</sup> and estimate the motion frequency up to 4–5 Hz,<sup>2,9</sup> meeting the requirements of a broad range of bridge types (flexible or rigid).

Many studies have been conducted on GPS structural monitoring,<sup>10–16</sup> aiming to determine the response and the main modal frequencies of structures.<sup>17,18</sup> Even though, in all the aforementioned applications, the GPS monitoring was generally successful for determining structure response at cm level, it faced challenges due to multipath effects in the GPS measurements from the structure elements (i.e., towers, cables and passing vehicles on the bridge<sup>19</sup>) and obstructions or signal interference producing cycle slips in the GPS measurements,<sup>20</sup> resulting in additional coloured noise and biases.<sup>21</sup>

Several studies focused on developing techniques to overcome the impact of the GPS monitoring error sources, by using adaptive filters (AFs),<sup>22</sup> or other filtering methodologies such as Chebyshev and Wavelet Transform,<sup>21</sup> to mitigate the multipath impact and reduce the GPS data noise. Another approach is to combine GPS data with other sensors in order to reduce the impact of the GPS data errors. For instance, the integration of accelerometer with GPS data, by applying Kalman filter, results to a displacement time series of low noise level<sup>23</sup> where the overall system (GPS and accelerometer) reliability and performance are improved. Robotic Total Stations (RTS) have been combined with GPS in order to reduce the GPS data errors<sup>7,24</sup> and mitigate the impact of the multipath effect in GPS data.<sup>19</sup> Also, in case of poor availability or poor GPS, satellite geometry is to use supplementary sensors such as pseudolites or localites.<sup>25,26</sup> However, potential inconsistencies between GPS and the other sensors (frequency bands, sampling rate, etc.) limits their integration.<sup>27,28</sup> Thus, the combination of GPS with other sensors cannot always lead to improvement of GPS displacement accuracy, as it strongly depends on the number of valid satellites and the geometry of the satellite constellation.

The development of other Global Navigation Satellite Systems (GNSS; GLONASS, Galileo, BeiDou) provides a complementary solution to overcome some of the limitations of using GPS alone for bridge displacement monitoring. It is broadly proved in previous studies that the combination of GPS with other GNSS constellations contributes in improving satellite geometry, due to the increased number of valid satellites,<sup>29–31</sup> and leads to the enhancement of the accuracy<sup>32–34</sup> and availability of GNSS solution.<sup>35,36</sup>

In this study, we investigate whether and under which conditions the contribution of GNSS systems can be beneficial and enhance the performance of GPS-only monitoring of the Severn Suspension Bridge, in the United Kingdom. The assessment of the GPS-only and multi-GNSS solutions is based on the quality of the displacement time series (i.e., noise level and availability) and the accuracy of the estimated modal frequencies. The GPS-only and multi-GNSS solutions and parameters expressing the quality of the satellite constellation and the satellite signals are analysed to form a methodology, which can define the solution (GPS-only or multi-GNSS) that leads to the most reliable estimation of the bridge response (displacement and modal frequencies). Part of this methodology is to simultaneously use also a zero-baseline measurements at the base-reference station during the monitoring period, in order to evaluate the quality of the GPS-only and multi-GNSS measurements and their noise level.

The beneficial contribution of GNSS to enhance GPS performance is well-known.<sup>29–35</sup> However, the main aim of the current study is to develop a methodology, which can be applied by non-experts of GNSS measurements, where the most reliable multi-GNSS solution will be defined and lead to the estimation of the bridge response characteristics (displacement and modal frequencies) without adopting any advanced GPS/GNSS processing techniques or integration of the GNSS receivers with other sensors. The main approach is to use standard GNSS processing techniques, such as double difference (DD), which can be easily configured and run in real time. Furthermore, even though the methodology was developed using the available satellite systems for the monitoring of Severn Bridge, in the United Kingdom, this methodology can be applied for the monitoring of any major civil engineering infrastructure (i.e., bridges, tall buildings, etc.) and use any available satellite system of the GNSS technology, according to the availability at the corresponding geographic area.

## 2 | METHODOLOGY

The developed method evaluates the performance of the GPS-only and multi-GNSS solutions in the bridge monitoring and how the multi-GNSS approach can resolve problems of the GPS-only solution, which is reflected in the displacement time series as higher noise level or poor availability (i.e., gaps) and reduced accuracy in the modal frequencies estimation. To evaluate the enhancement which can be achieved by including other satellite systems, zero-baseline measurements need to be conducted, where two GNSS receivers are connected with the same antenna; one used as base-reference station and the other as rover. The main advantage of the zero-baseline measurements is that most of the error sources of the GNSS records are cancelled through the DD processing mode. Hence, the GPS/GNSS zero-baseline time series vary around zero, expressing the impact of the errors due to the geometry of the satellite constellation, amplified by the receiver noise.<sup>35</sup> The zero-baseline measurements are an approach which has been adopted in many studies for the modelling of the GPS receivers noise and the impact of the satellite constellation.<sup>37,38</sup> In our study, the GNSS base station, apart from reference station for the GNSS stations deployed on the bridge, was also connected to a second GNSS receiver to carry out the zero-baseline measurements.

For the assessment of the noise level and availability of the GPS/GNSS solution, the different solutions (GPS and multi-GNSS) were related to parameters which express the quality of the measurements. More specifically, those parameters are (i) the geometric dilution of precision (GDOP) which expresses the quality of the geometry of satellite constellation of each measurement<sup>39,40</sup> and (ii) the signal-to-noise ratio (SNR), which reflects the quality of the satellite signals and can be used to identify problematic satellites, signal interference and cycle slips.<sup>35,41</sup> Furthermore, the multipath parameter (MP), which can be computed by applying a linear combination between the code and carrier phase measurements of GNSS dual frequency receivers,<sup>39</sup> can be used for the detection of cycle slips which are caused by strong multipath environment and site-specific effects. Both detections (MP and cycle slips) were used.

For the processing of the bridge GPS/GNSS records, the DD mode was used with the GNSS reference station used as base, in order to be consistent with the zero-baseline measurements processing and limit the error sources of the GNSS bridge measurements. Error sources, such as troposphere and ionosphere, are significantly limited due to the relatively short baseline (<1 km).<sup>42,43</sup> However, the impact of the multipath effect, which depends on the site-specific surrounding conditions for each station,<sup>44</sup> remains the main error sources of the bridge GNSS stations.

To assess the effectiveness of the developed method, an additional step was introduced in this study, where the displacement time series and the modal frequencies deriving of the GPS-only and multi-GNSS solutions were assessed. The comparison aims to examine whether the characteristics of the response deriving from the multi-GNSS time series are significantly more accurate and reliable by using the multi-GNSS approach for the time intervals of the weak GPS-only solution.

## 3 | SEVERN BRIDGE MONITORING

The Severn Suspension Bridge, which is one of the largest suspension bridges in the United Kingdom, was monitored to assess the multi-GNSS monitoring approach. The bridge, which was opened in September 1966, carries the M48 motorway as a dual carriageway over the Severn Estuary, connecting the Bristol area to South Wales.<sup>45</sup> The bridge's deck is supported by two main cables and hangs between two steel towers. Its length is 1600 m, consisting of a central suspended main span of 988 m in length, which is supported by the two towers, through the cables. Each tower has a height of 136 m above mean sea level.<sup>46,47</sup>

Apart from the GNSS monitoring campaign of 2015, on which the current study was based, there was also the GNSS monitoring campaign of 2010. Previous studies of monitoring Severn Suspension Bridge, which were based on both GNSS monitoring campaigns (2010 and 2015), have revealed that the main modal frequencies of the midspan are 0.147 and 0.226 Hz, at the vertical component, and  $\sim 0.09$  Hz at the lateral component, while for the tower, the main modal frequency is 0.147 Hz on the longitudinal component, which reflects the impact of the first mode of the deck on the towers.<sup>46,48</sup> Regarding the vertical response at the midspan, it can reach 10–20 cm, depending on the vehicle loading, and the longitudinal/lateral response of the towers may reach even up to 2 cm.<sup>11,45,46,48</sup>

### 3.1 | Deployment of GNSS stations

The monitoring of Severn Bridge was conducted between the 20 and 23 July 2015, focusing on 11 monitoring points of the bridge (Figure 1). Table 1 presents the GNSS receivers and antennae models at each monitoring point and the corresponding recording time period. A GNSS station was installed on the roof of the toll building,  $\sim 1$  km away from the eastern tower of the bridge, which was fixed and used as base-reference station. The GNSS stations at some monitoring points on the bridge consisted of a choke ring antenna (Leica AT504) to reduce the multipath effect. All the GNSS receivers were recording with a sampling rate of 10 Hz.

For the scope of this study, the analysis was focused on points T1 and T2 of the east tower and the points B and F at the midspan. Those points were chosen as they express the response of two crucial elements of the bridge (i.e., the tower of the bridge and the deck at the midspan), while the impact of the multipath effect is expected to vary between the two locations; the points at the tower are less affected by multipath due to the open-sky and unobstructed environment relatively to the midspan, where the surrounding structural elements (e.g., towers and cables) create a complex multipath environment. Furthermore, the midspan GNSS stations are also expected to be affected by dynamic multipath conditions, which is produced by the passing vehicles (i.e., high lorries<sup>41,49</sup>). However, the use of choke-ring antennae at the locations B and F and mounting the GNSS antennae on poles  $\sim 5$  m above deck level restricts significantly the reception of reflected signals from the vehicles and limits the impact of the dynamic multipath.

At the base station two GNSS receivers, a Leica GR10 and a Leica GS10 were connected via a splitter (Gems GPS 2-way splitter GS12) to a single Leica AR-10 choke ring antenna with ray dome to form the zero baseline. The GNSS measurements of the zero baseline are mainly contaminated by errors due to the geometry of the satellite constellation and the receiver noise.<sup>35</sup> The GNSS measurements of zero baseline were conducted during 44 consecutive hours, starting at 12:00 AM on 20 July 2015 until 08:00 AM on 22 July 2015 (Table 1). Then, the base station was restricted on Leica GR10 after moving GS10 to a handrail location on the bridge.

The available GNSS satellites at the geographic area of Severn Bridge during the monitoring period were GPS, GLONASS, Galileo and BeiDou. However, due to the limited number of visible BeiDou satellites (i.e., one or two satellites observed for short duration) and the fact that only three Galileo satellites were in operation at that time,

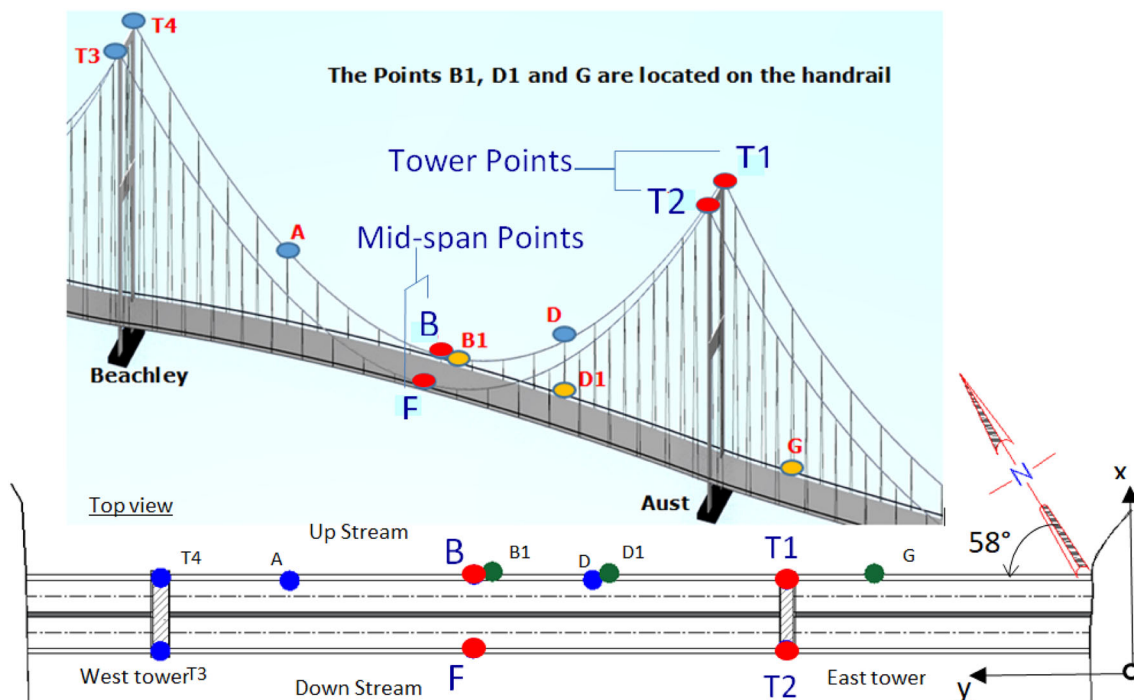


**FIGURE 1** The location of the GNSS stations on the bridge and the plan view of the bridge with the corresponding angle, with respect North, which is applied for the transformation of the coordinate system to the bridge local coordinate system (longitudinal— $y$ -axis, lateral— $x$ -axis and vertical— $z$ -axis). The east tower points (T1 and T2), the midspan points (B and F) and the points A and G, which are analysed in the current study, are highlighted (red circles)

TABLE 1 Specifications of GNSS stations for the Severn Suspension Bridge monitoring

Group	Points	Antenna type	Receiver type	Time period for collecting GNSS data			
				20 July	21 July	22 July	23 July
Base*	Ref.	Leica AR10	Leica GS10	12:00–24:00	00:00–24:00	00:00–24:00	00:00–09:00
	R-b		Leica GR10	14:22–24:00	00:00–24:00	00:00–08:15	x
Tower	<b>T1</b>	<b>Leica AS10</b>	<b>Leica GS10</b>	<b>14:22–24:00</b>	<b>00:00–24:00</b>	<b>00:00–24:00</b>	<b>00:00–08:16</b>
	<b>T2</b>	<b>Leica AS10</b>	<b>Leica GS10</b>	<b>14:22–24:00</b>	<b>00:00–24:00</b>	<b>00:00–24:00</b>	<b>00:00–08:16</b>
	T3	Leica AT504	Trimble Net9	12:10–24:00	00:00–24:00	00:00–24:00	00:00–09:00
	T4	Leica AT504	Trimble Net9	12:19–24:00	00:00–24:00	00:00–24:00	00:00–09:00
cables	<b>A</b>	<b>Leica AT504</b>	Javad <b>Leica1200</b>	13:24–24:00	00:00–03:32 20:30–24:00	<b>00:00–11:16</b> <b>16:32–24:00</b>	<b>00:00–09:00</b>
	<b>B</b>	<b>Leica AT504</b>	<b>GS10 Leica1200</b>	x	<b>09:18–11:00</b>	<b>00:00–24:00</b>	<b>00:00–09:00</b>
	D	Leica AT504	Javad	x	12:40–24:00	00:00–04:55	00:00–09:00
	<b>F</b>	<b>Leica AT504</b>	<b>Leica GS10</b>	<b>14:22–24:00</b>	<b>00:00–24:00</b>	<b>00:00–24:00</b>	<b>00:00–08:16</b>
Handrail	B1	Leica AS10	GS10 Leica1200	x	03:03–20:25	x	x
	D1	Leica AS10	Leica GS10	15:36–24:00	00:00–02:45	x	x
	<b>G</b>	<b>Leica AR10</b>	<b>Leica GS10</b>	x	<b>00:00–24:00</b>	<b>09:18–24:00</b>	<b>00:00–09:00</b>

Note: The GNSS data of (a) the base station, (b) the points T1 and T2, of the east tower, and (c) the points B and F of the midspan are primarily used in the current study. Data of points A and G which fulfilled the criteria of the study were also analysed to validate the results of the other points. The antenna of the base station was connected to two GNSS receivers to form the zero baseline. The Leica AT504 antenna is a chock-ring reducing the multipath effect and used for the critical monitoring points of the cables and the towers. The points in bold are used in the current study and with x symbol are identified the periods with no available data.

BeiDou and Galileo constellations had a marginal effect on the positioning performance. Hence, only GPS and GLONASS constellations are used to evaluate the performance of multi-GNSS solutions. Furthermore, as there were more than one type of receiver, the evaluation of the performance was restricted to use only Leica receivers, as the ambiguity resolution of the GLONASS measurements in DD mode requires receivers of the same type due to the inter-frequency bias (IFB).<sup>50</sup> In addition to the GNSS data, other meteorological data, including air temperature and bridge's steel temperature, relative humidity, wind speed and wind directions, were gathered during the survey at specific locations. However, the analysis of the meteorological data and their correlation with the GNSS data were not in the scope of this study, and hence, they were not used.

## 4 | DATA PROCESSING

The GNSS records were downloaded from the receiver on a periodic basis, and they were processed (zero baseline and bridge monitoring measurements) using RTKLIB v2.4.2.<sup>51</sup> By introducing the GNSS records to the software, preprocessing analysis was made where potential epochs or time intervals of cycle slip and low quality of satellites signal (due to multipath, signal interference, etc.) were identified. However, those time intervals were related or coincided with periods of relatively high GDOP values and where further analysed at the GPS-only/multi-GNSS time series analysis stage.

To analyse the response of the bridge, the data have been post-processed in a kinematic mode using the DD technique using dual frequencies (L1 and L2) measurements for short baseline (~1 km long). The processing was based on broadcast ephemeris with a 15° cut-off elevation angle for different GNSS constellations. The kinematic positions at each monitoring station of the bridge and the zero baseline were computed relative to the reference point at the fixed GNSS base station.

In the RTKLib software, there are three strategies to fix the ambiguities during the kinematic post-processing of the GNSS records: (i) fix and hold, (ii) continuous and (iii) instantaneous.<sup>51</sup> The continuous and fix and hold strategies use the approach of Kalman filtering, while the instantaneous strategy uses an integer least squares method to fix the ambiguity epoch by epoch.<sup>51</sup> For the purpose of this study, the instantaneous was applied, as it is a more common

approach adopted by similar GNSS records processing software (e.g., Bernese<sup>52</sup>), especially when the GNSS records are not integrated with other sensors. Also, this approach is more easily applied for real-time monitoring application, such as the GPS bridge monitoring. However, in some cases, the fix-and-hold strategy was also applied to examine the impact of the Kalman-filtering approach and its potential enhancement on the GPS/multi-GNSS solution.

Due to the large amount of data, the GPS/GNSS data were split and processed in hourly intervals. To be consistent, the GPS/GNSS solutions of the different intervals were computed with respect to the coordinates of the GNSS base station, which derived from the zero-baseline measurements processing in static mode. Finally, the GPS/GNSS data of 10 Hz processing resulted in 3D coordinates kinematic time series in NEU relative to the fixed GNSS base-station coordinates.

Furthermore, for the bridge monitoring points, the 3D GNSS coordinates (E, N and U) were transformed, by using a linear transformation, into the local bridge coordinate system (lateral— $x$ , longitudinal— $y$  and vertical— $z^2$ ). For this purpose, the positions of tower points were used, as they represented the alignment of the bridge, to define the orientation of the bridge's longitudinal axis. The GNSS coordinate system was rotated by  $58^\circ$  anticlockwise, and the  $x$ -axis and  $y$ -axis expressed the lateral and longitudinal axis, respectively, while the  $z$ -axis expresses the vertical axis of the bridge (Figure 1).

## 5 | ZERO-BASELINE ANALYSIS

Since only the GPS and GLONASS satellite systems were used, the investigation was applied for three GNSS solutions: (i) GPS-only, (ii) GLONASS-only and (iii) multi-GNSS, combining GPS and GLONASS. The zero-baseline measurement analysis aims to reveal time intervals of low precision or availability of GPS-only solution and examine whether GLONASS contributes beneficially and results to a multi-GNSS solution of better precision than the GPS-only solution. Also, it was checked whether the GPS-only/multi-GNSS precision was strongly related with the corresponding GDOP, as it was proved by Msaewe et al.<sup>35</sup>

Since the GPS satellite constellation has a daily repetition (with a time lag of  $\sim 4$  min), any periods of weak GPS satellite geometry and problematic GPS satellites will be revealed in the 24-h time series. These identified periods will have mainly impact on the precision of the GPS-only solutions, which should also be reflected in the estimation of the displacement time series of the bridge monitoring points. Hence, even the zero-baseline measurements lasted 40 h, we analysed the 24-h zero-baseline measurements (21/07); any periods of weak GPS constellation observed in that time series will be also identified in any of the following days, by shifting the time period by multiples of 4 min, depending on the number of the days.

Figure 2 illustrates the GPS-only, GLONASS-only and multi-GNSS time series of the zero-baseline measurements and the time series of the corresponding GDOP values, where it is obvious that the GLONASS-only time series (N,E,U) have the highest deviation, expressing the high noise level. The GPS-only solution has significantly lower level of deviation, with some time intervals of higher noise level (for instance 01:00–02:00, 08:00–09:00, 11:00–12:00 and 12:00–13:00) which coincide with relatively high GDOP values for the GPS satellite constellation. For some of those time intervals, the high GDOP value is the result of low GPS satellite number (Figure 3; e.g., 08:00–09:00 with even 4 GPS satellites) or relatively low number of GPS satellites but probably weak geometry (e.g., 12:00–13:00 with 6 satellites but GDOP value reaching 9). For those time intervals, the multi-GNSS solution leads to a more precise time series, thanks to the increased number of satellites and the significantly improved geometry of satellite constellation, reflected on the corresponding GDOP value. Also, the main improvement of the multi-GNSS solution is achieved on the Northing component, for which the GPS-only solution is weak for GPS measurements of high latitude,<sup>53,54</sup> and on the vertical component, which is the most susceptible to high noise level. The relationship between GDOP value and the measurements precision is known and investigated thoroughly in Msaewe et al.,<sup>35</sup> where it was shown that the precision is reversely proportionally to GDOP for values larger than 2. For smaller values of GDOP, the satellite constellation does not have significant impact on the measurement precision.

Furthermore, to assess the precision of the GNSS solution, the root-mean-square (RMS) error derived from the 1-h interval data processing was computed for the three examined solutions (Figure 4). It is obvious that the GLONASS-only solution is the least precise, with significant high noise in the vertical component. Regarding the GPS-only and multi-GNSS solutions, it is observed that they are of similar precision and confirmed that the multi-GNSS solution is more precise mainly for the North component, where the GPS-only solution is weak due to the poor geometry of satellite constellation for high latitude locations, especially for the time periods 08:00–09:00 and 11:00–12:00 when the number of GPS satellites is relatively low (i.e., ranging between 4 and 7; Figure 3).

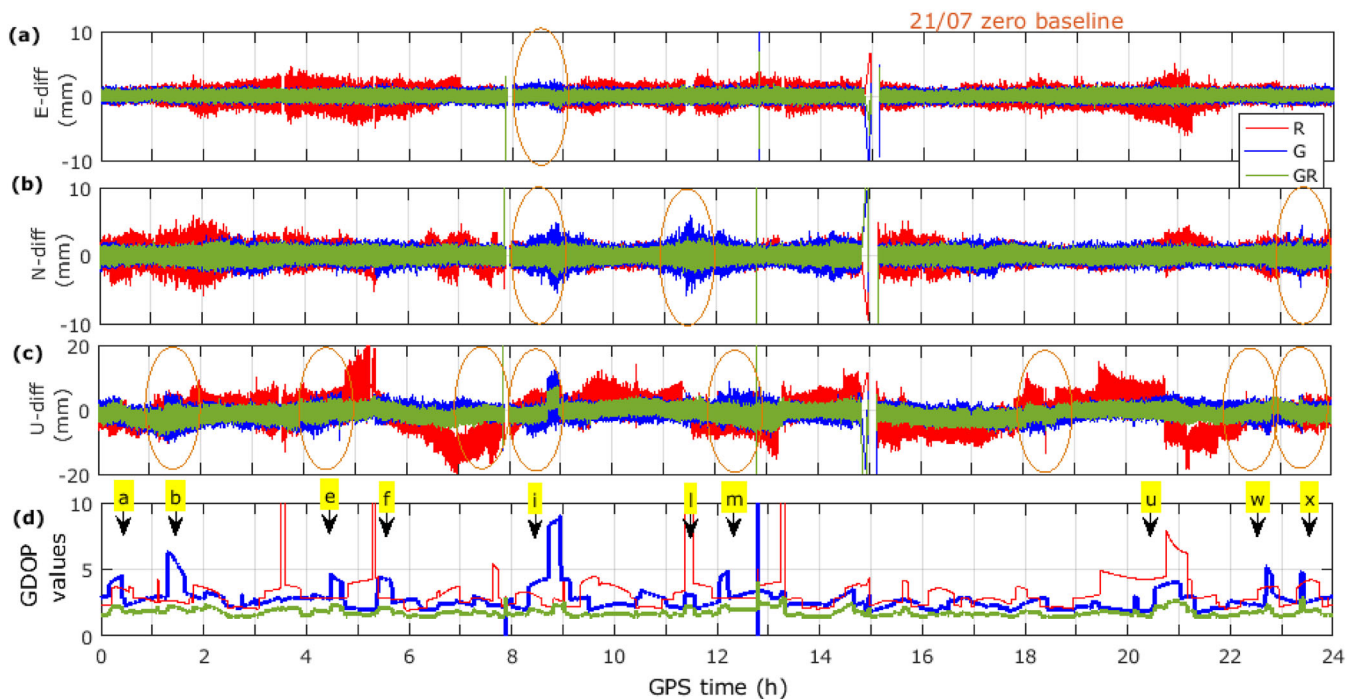


FIGURE 2 (a–c) Coordinate time series of the zero baseline showing the noise level for the GPS-only (blue), GLONASS-only (red) and multi-GNSS (GPS + GLONASS; green) solutions and (d) the corresponding GDOP values on 22 July 2015. The periods of strong correlation between the high GDOP values and the high deviation of the corresponding satellite constellation solution (included in circles) are obvious

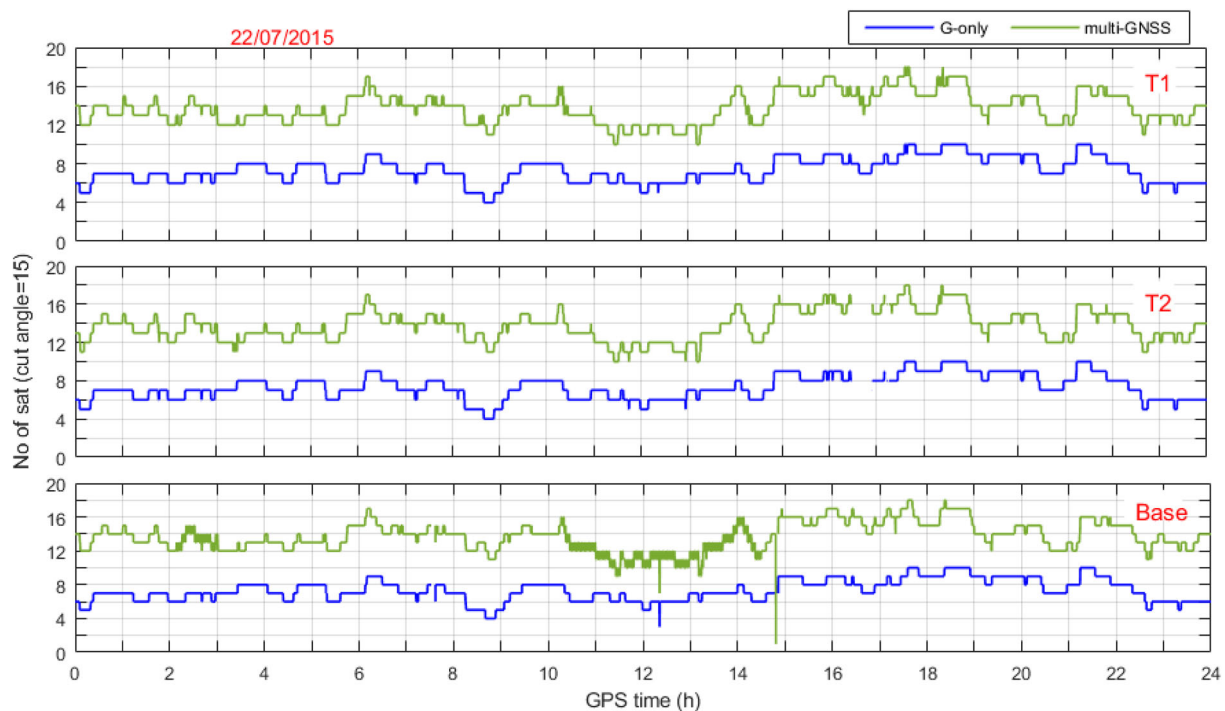


FIGURE 3 Number of visible GPS and multi-GNSS (GPS + GLONASS) satellites as they are tracked by the GNSS receivers at the locations of (top) point T1, (middle) point T2 and (bottom) base station on 22 July 2015. In general, the same number of satellites are tracked by all receivers. The receivers of the tower seem to have more stable tracking of satellites for the period between 12:30 and 14:00, potentially due to better visibility. It is also observed that the number of GPS satellites drops down to four, which is reflected in very high GDOP values (GPS GDOP  $\sim 9$  for interval 08:40–08:55 in Figure 2)

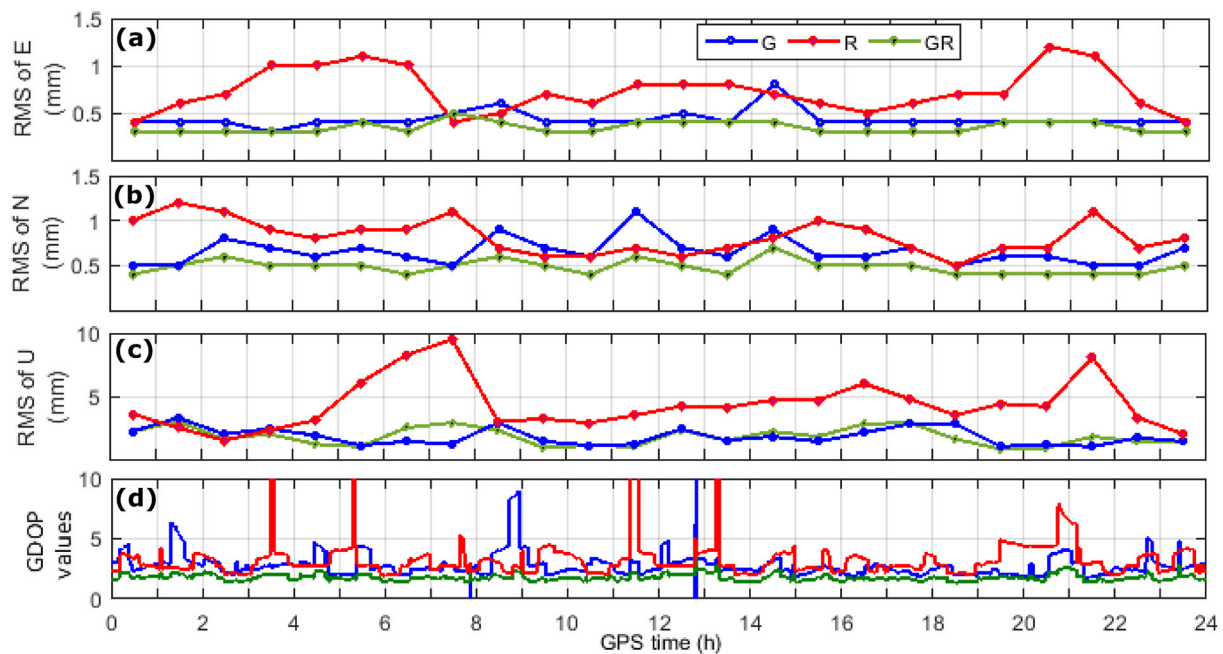


FIGURE 4 Comparison of precision expressed as RMS for GPS-only (G), GLONASS-only (R) and multi-GNSS (G + R) along zero baseline components and the corresponding time series of GDOP values for each satellite constellation. It is observed that multi-GNSS solution has generally the lowest RMS values, slightly better than the GPS-only solution, apart from some limited periods of weak GLONASS solution (i.e., 6–8 h in the U component)

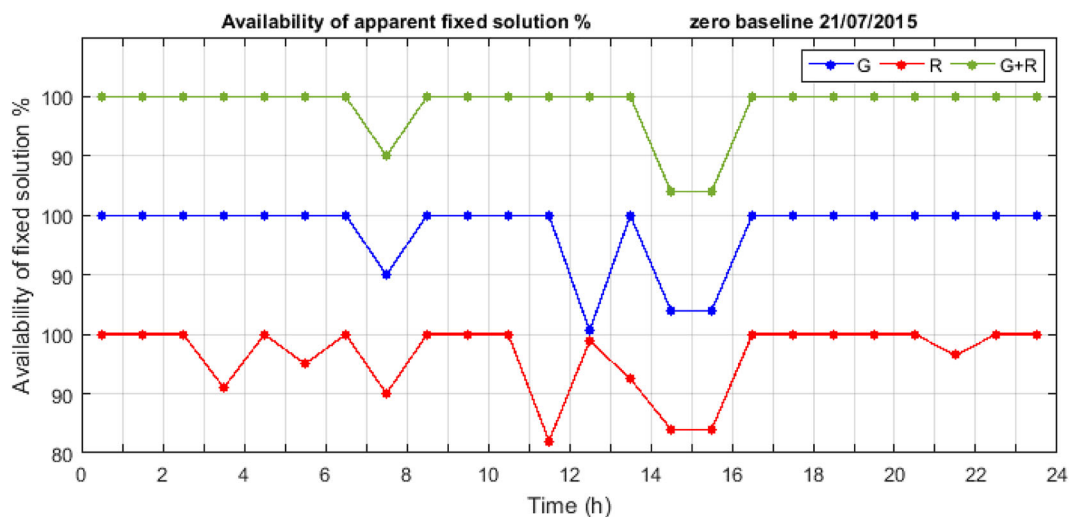


FIGURE 5 The fixing rate availability of apparent of GPS-only (G), GLONASS-only (R) and multi-GNSS (G + R) along zero baseline solution on 21 July 2015. The multi-GNSS solution has the highest availability in terms of fixed solution

Regarding the availability of the three solutions (Figure 5), the multi-GNSS processing leads to the solution with the highest availability, which during the 24-h period of 21 July is 100%, apart from the three time intervals (07:00–08:00, 14:00–15:00 and 15:00–16:00), where it reached 90%, 84% and 84% of availability due to gaps of 6, 10 and 10 min, respectively. Those gaps were produced due to unrecorded data by one of the two reference receivers. The GPS-only solution is of lower availability than multi-GNSS, dropping lower than 90% for some 1-h periods and reaching even below 81% for the time interval 12:00–13:00 due to the limited number of GPS satellites (i.e., reaching even three satellites; Figure 3). The GLONASS-only solution proved to be of lower availability as illustrated in Figure 5.



Based on the analysis of the zero-baseline measurements, it can be seen that the multi-GNSS solution is generally of higher accuracy and availability of that of the GPS-only solution. However, the main enhancement in the solution is achieved for the time periods of relatively low GPS satellites number and high GDOP values of the GPS-only solution, which reflects the influence of the poor GPS satellite constellation on the quality of the GPS solution.

## 6 | SEVERN BRIDGE MONITORING ANALYSIS

The investigation of the accuracy of GPS-only and multi-GNSS solutions focused on the analysis of the points which (i) had GNSS receiver compatible with the base station, allowing to fix the GPS/GLONASS ambiguity resolution, and (ii) with available 24-h data records if possible, in order to assess the GPS satellite constellation. Based on these criteria, the analysis was based primarily on (i) the Eastern Tower (T1 and T2) and (ii) the midspan (B and F). The GNSS data of the points A and G were also analysed, in order to validate the outcome of the midspan points. Furthermore, the point C GNSS data of 2010 GNSS monitoring campaign were also analysed to evaluate the beneficial contribution of multi-GNSS for a period of (i) different environmental/weather conditions (March 2010 against July 2015) and (ii) different GLONASS satellite constellation.

The GPS-only and multi-GNSS displacement time series were assessed based on the criteria of the availability and the noise level of the derived displacement time series and the reliability of the estimated modal frequencies. The time series were split into low- (<0.1 Hz) and high-frequency (>0.1 Hz) components, in order to evaluate the impact of the noise level of the GPS-only/multi-GNSS measurements for different frequency bands. Eighth-order Chebyshev I high- and low-pass filters were used as it has been applied successfully in previous studies of GPS bridge monitoring applications.<sup>8,41</sup> The cut-off frequency of 0.1 Hz was selected as the multipath effect is mainly limited to frequencies below 0.1 Hz.<sup>41</sup> In the following sections, we present representative cases of time periods where (i) the GPS and multi-GNSS solutions have same level of accuracy thanks to the high-quality of GPS measurements and the GLONASS constellation which cannot have any beneficial contribution to the solution and (ii) cases where the multi-GNSS solution proved to be beneficial, with respect the GPS-only solution, for the reliable estimation of the bridge response.

### 6.1 | Eastern Tower monitoring analysis

The displacement time series of the GPS-only solution of station T2 were characterised with more gaps than the corresponding time series of T1 station. Even though both stations at T1 and T2 are occupied by similar Leica receivers, the positioning performance may differ at specific intervals due to the impact of the different surrounding environment at the two locations, which affects the availability of fixed solution (Table 2). To enhance the positioning solution, a multi-GNSS solution was applied to increase the number of satellites and tackle the problem of poor satellite availability and potential multipath effect and thus reduce the gaps in the fixed solution (Table 2). This proves that a combined solution can overcome problematic periods as well as reducing the noise level.<sup>55</sup>

Figure 6 illustrates the lateral, longitudinal and vertical response of T1 and T2 for the 24-h period (22 July) and the corresponding GDOP values of the GPS-only/multi-GNSS satellite constellations. Similarly to the zero-baseline measurements (Figure 2), it is obvious that for the periods of relatively high GDOP values for GPS constellation, the GPS-only displacement time series is characterised by significantly higher deviation in the lateral (periods: i, j, l, r, u), longitudinal (periods: i, l, r) and vertical (periods: b, i, j, m, r, u, w) components, which indicate higher noise. The time intervals of GPS-only solution of high noise level coincide with most of those of the zero-baseline measurements and could be the result of the weak satellite geometry or poor GPS satellite signals.

**TABLE 2** Comparison of percentage of fixed solution availability at T1 and T2 between GPS-only and multi-GNSS solutions

Interval	Availability sol. % at T1		Availability sol. % at T2		Problematic satellite at T2
	GPS-only	Multi-GNSS	GPS-only	Multi-GNSS	
(i) 08:00–09:00	100	100	66.9	92	G15
(l) 11:00–12:00	99.8	99.9	71.6	94	G21
(q) 16:00–17:00	99.8	100	75.4	87.3	G26

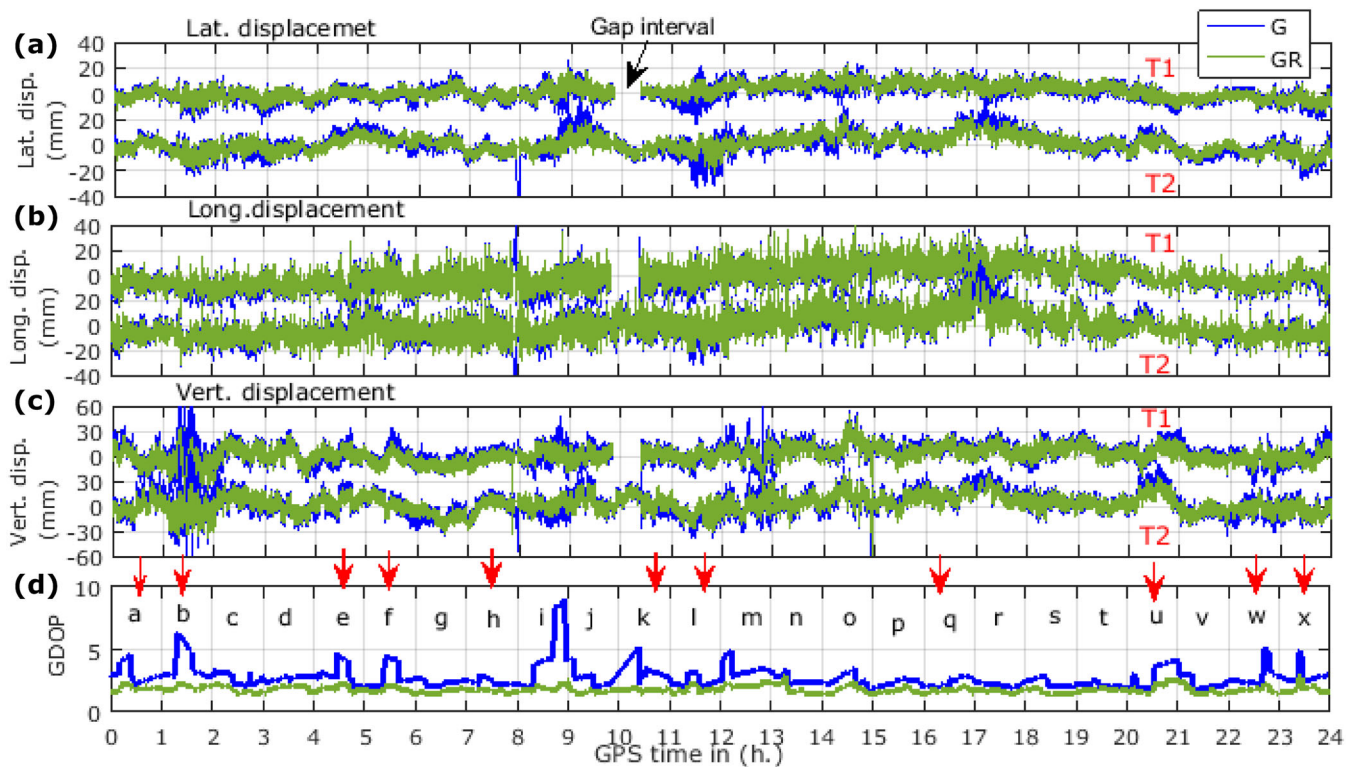
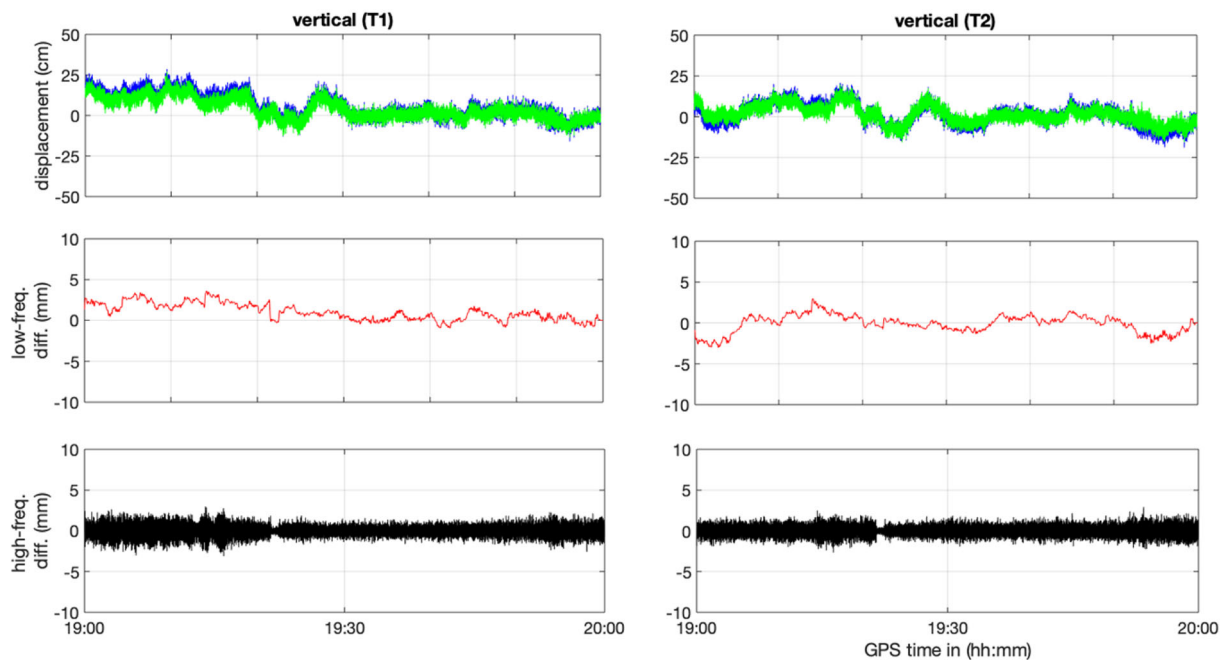


FIGURE 6 (a–c) Displacement time series at tower points T1 and T2 showing the comparison between the GPS-only and multi-GNSS solutions and (d) the corresponding GDOP values with GPS-only and multi-GNSS on 22 July 2015. It is evident the larger deviation of the displacement of the GPS-only solution for the periods of high GDOP values relatively to the less noisy multi-GNSS solutions

A representative case where the GPS and multi-GNSS solutions led to similar displacement time series is for the time interval between 19:00 and 20:00 (Figure 7), due to the relatively high number of GPS satellites ( $>8$ ; Figure 3) and strong geometry of the GPS satellite constellation (GPS GDOP  $\sim 2$ ; Figure 4). It is evident that the difference between the GPS and multi-GNSS solutions ranges up to a few mm for both low- and high-frequency time series of the vertical component. The same difference between the time series of that time interval was also observed for 20 and 21 July, proving that the high quality of GPS measurements thanks to the strong geometry of GPS satellites is repeated daily (with a time lag of  $\sim 4$  min), and additional GNSS satellites do not enhance further the accuracy of the solution for the specific time interval.

On the contrary, for the time interval between 01:00 and 02:00 is evident the higher noise level in the vertical component of the GPS-only solution, with respect the multi-GNSS solution, especially for the period between 01:14 and 01:34; the latter is related to the high VDOP value (vertical DOP) of that time interval (Figure 8). In that case, the GPS constellation consists of six satellites with VDOP value ranging between 5 and 3.5, while the multi-GNSS consists of 13 satellites much more uniformly distributed, which results to VDOP below 2. The poor GPS satellite constellation produces the high noise level in the GPS-only solution and results to deviate from the multi-GNSS vertical displacement even up to 4 cm for the time interval. The impact of the poor GPS satellite geometry is significant on the low-frequency component of the displacement, as the difference between the low frequency of GPS-only and multi-GNSS solution is larger, reaching up to 2.5 cm, whereas for the high-frequency component ranges around  $\pm 1$  cm. Apparently, the contribution of the GLONASS satellites, by covering the Northern part of the sky, limits the impact of the surrounding obstructions and augments the multi-GNSS solution as it is reflected in the accuracy of the estimated displacement time series. The difference seems to be higher in the low-frequency component, as the multipath errors and satellite constellation problems correspond to the low-frequency band of the GNSS measurements. Similar behaviour of the GPS-only and multi-GNSS solutions is observed for the same time interval of 21 and 23 July.

Likewise for the time interval between 08:00 and 09:00, the number of GPS satellites reduces from eight to five (08:15) and then to four satellites (08:40–08:55; Figure 9). The poor geometry of GPS satellite constellation in that time interval leads to gaps in the GPS solution and significant difference from the multi-GNSS solution for the T1 and T2



**FIGURE 7** (Top) Displacement time series of the vertical component of points T1 and T2 and the derived (middle) difference of the low frequency between the solutions of GPS-only and multi-GNSS and (bottom) the difference of the high-frequency component between the GPS-only and multi-GNSS solutions for the time interval between 19:00 and 20:00 on 22 July

stations. The difference of the low- and high-frequency components between the two solutions increases when the GPS GDOP value decreases, as the errors due to weak GPS satellite constellation are greater for high GDOP values and the deviation larger from the multi-GNSS solution. Characteristically, at around 08:50 when the GPS GDOP value is greater than 8, the differences in the low- and high-frequency components reach up to 20 mm (Figure 9). Furthermore, the data gaps observed in the GPS solution of point T1 for the period between 08:00 and 08:20 are probably due to poor quality of some of the GPS satellite signals, since both T1 and T2 receive signals from eight satellites. This is a site-specific effect and caused by the surrounding environment of station T1 and potential multipath effect. A similar problem is observed in the period from 11:00 to 12:00, where the GPS-only solution for the lateral displacement of stations T1 and T2 is less precise for the period 11:22–11:34, when the GPS constellation DOP value increases (Figure 10). However, a significantly higher noise level of the GPS solution is observed at the T2 station around 11:50, where the difference between GPS-only and multi-GNSS solutions reaches up to 20 mm in the low- and high-frequency component. This is due to the poor satellite signal of satellite G21, which starts coming over the horizon at around 11:40, but the signal received by this satellite is of very low quality due to the low elevation angle-related atmospheric and multipath noise, according to the SNR and MP parameters of the GNSS receiver record at T2; the SNR of L1 and L2 is very low for G21 ranging  $\sim 35$  and  $\sim 24$  dBHz, respectively, while the MP2 fluctuation exceeds 1 m. Those parameters indicate potentially a very strong multipath effect for station T2 for that satellite, with a large impact on the accuracy and precision of the GPS-only solution. The SNR of G21 is also slightly increased for station T1 but apparently not significantly enough (still SNR1 ranging at  $\sim 45$  dBHz and SNR2  $> 35$  dBHz) to have an impact on the GPS-only solution (Figure 10). However, the multi-GNSS solution results to a displacement time series of consistent noise level of that of station T1, even without excluding the G21 satellite from the processing, indicating the benefit of using multi-GNSS solution in unfavourable conditions.

## 6.2 | Severn Bridge midspan monitoring analysis

The potential high noise level of the displacement time series is not that evident in the GPS-only solution for the midspan due to the relatively large response amplitude, especially for the vertical component. In Figure 11, the difference between the performance of GPS-only and multi-GNSS solutions is not obvious. However, by calculating the

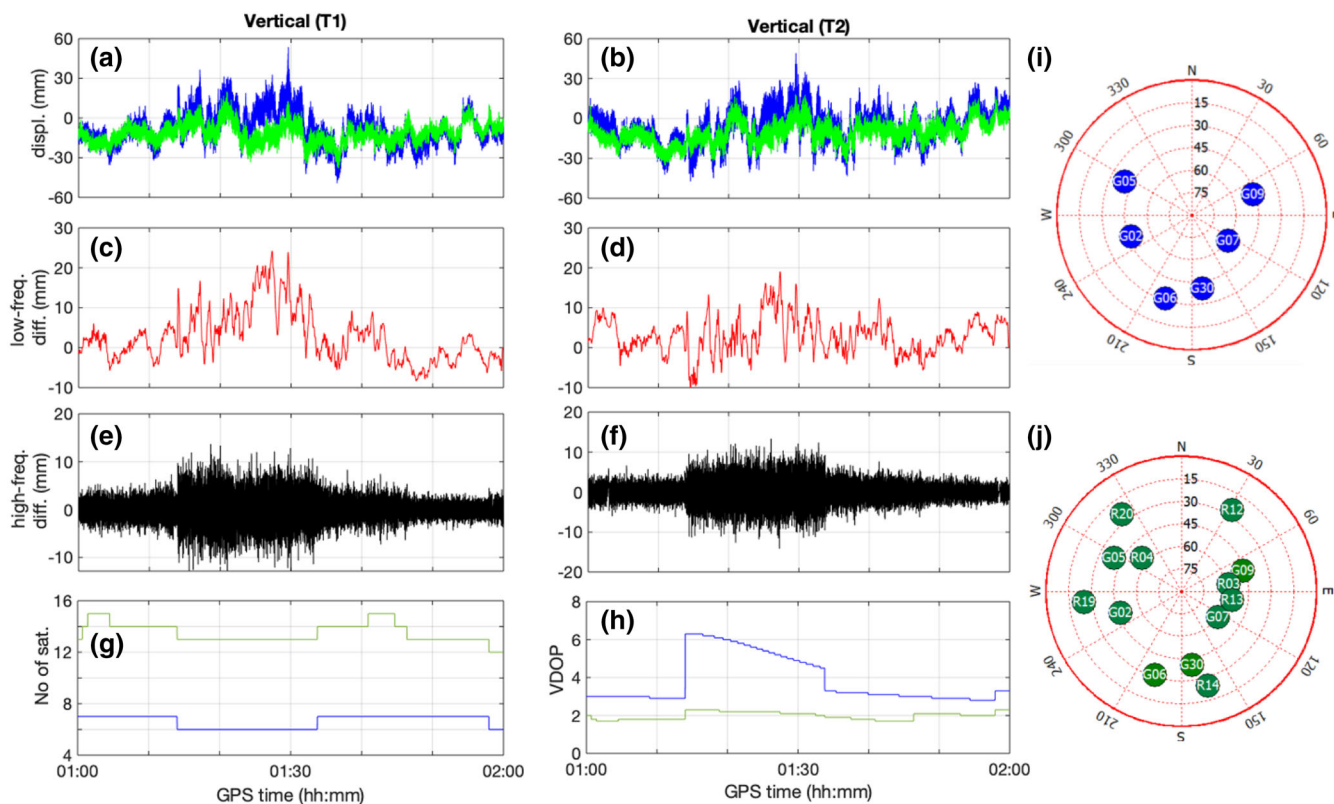


**FIGURE 8** The GPS-only (blue) and multi-GNSS (green) vertical displacement for (a) Tower T1 and (b) T2 and their differences between the corresponding (c,d) low-frequency and (e,f) high-frequency components. For the period between 01:14 and 01:34, there is a slight reduction of the available GPS satellites (from seven to six) (g) and a significant increase of the VDOP values (h). In the skyplots is evident the difference in the satellite geometry between the (i) GPS-only and (j) multi-GNSS constellation for this 1-hour time period. It is evident the high deviation of the GPS-only displacement time series, relatively to the multi-GNSS displacement time series, due to the reduction of the GPS satellite number, reflected also in the VDOP value

difference between the two solutions, it is clear that the deviation of the difference is increased mainly for the periods where the GDOP value of GPS constellation is significantly higher than that of multi-GNSS constellation (Figure 12). These intervals are the same which are characterised as GPS-only low-precision intervals from the zero-baseline measurements (Figure 2). The problems which are faced on the stations on the cables (B and F) are similar to those of the Eastern Tower (T1 and T2): poor GPS satellite constellation, poor quality of GPS satellite signal and multipath effect. However, the structural elements (cables and towers), which are at higher levels than stations B and F at the midspan, create stronger multipath environment than that of the stations at the towers.

In Figure 13, the GPS-only and GNSS solution for stations B and F in the vertical components are presented. Similar to the vertical components of the tower stations (T1 and T2, Figure 9) at the same interval, the low quality of the GPS-only solution for the time period between 08:20 and 08:55 was expected due to the poor GPS satellite constellation. However, the GPS-only solution of stations B and F shows significantly more gaps which are produced due to the obstructions of the satellite signals of the already limited number of satellites, which lead to low availability for the GPS-only solution. The time period the GPS-only solution availability is 49% and 69% for the stations B and F, respectively, while the multi-GNSS solution is 100% for both stations. The lower availability at station B is probably due to the position of station B at the northern side of the midspan of the bridge, which probably restricts the visibility of the available GPS satellites with azimuth between  $120^\circ$  and  $300^\circ$ . The multi-GNSS constellation covers more broadly and uniformly the open sky having continuously available more than 11 satellites. Thus, the weak GPS constellation leads to a poor solution with several gaps in the position solution and differs from the estimated lateral displacement of the multi-GNSS solution up to 50 mm in both the low- and high-frequency components.

Furthermore, during the interval of 11:22–11:34, the VDOP is slightly increased (i.e., up to 2) following the trend of the GDOP for the T1 and T2 stations (i.e., larger than 3, Figure 10). However, the GPS-only solution has gaps which

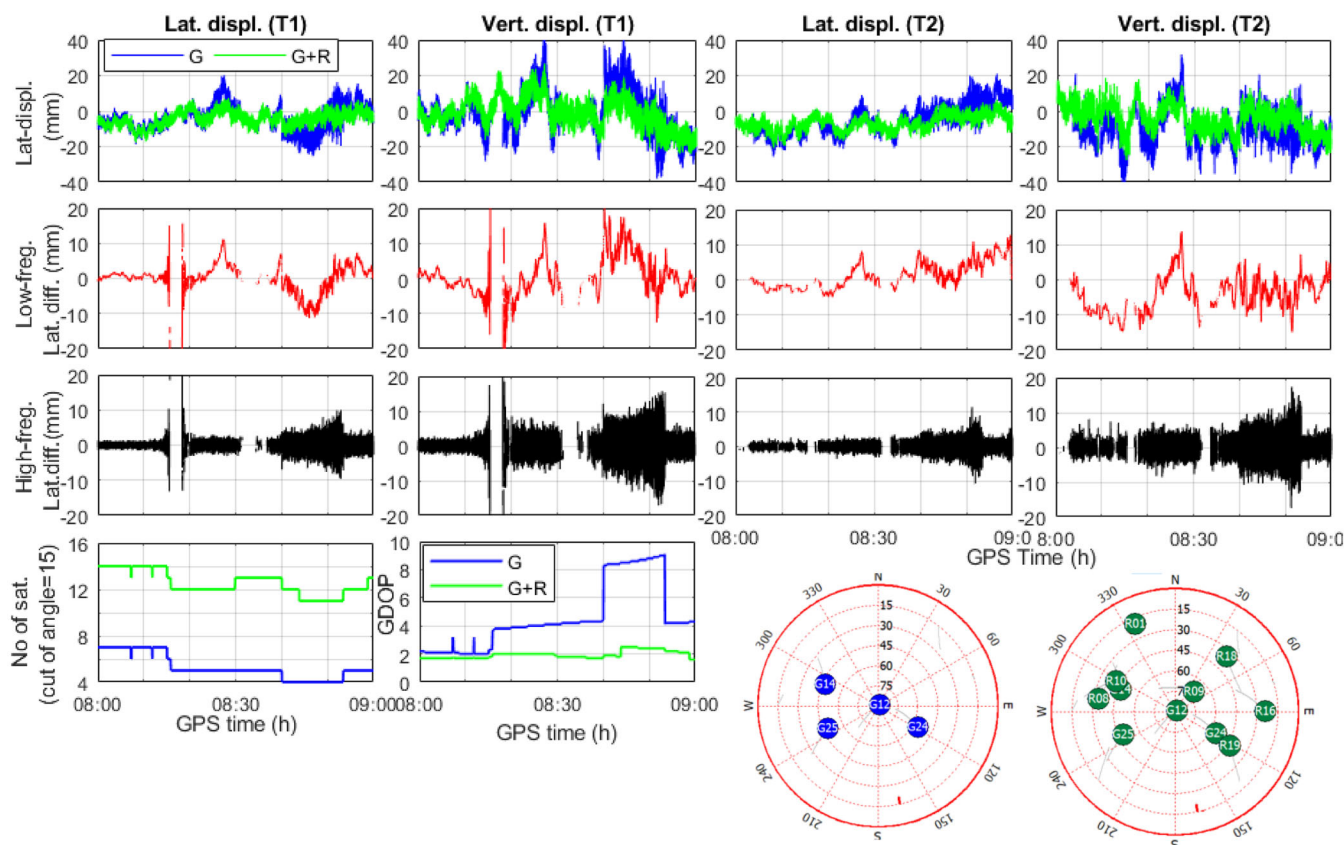


**FIGURE 9** The GPS-only and multi-GNSS displacement of the lateral and vertical components for T1 and T2 with the differences of their corresponding low- and high-frequency components. The time series of the number of satellites of GPS and multi-GNSS constellation and the corresponding GDOP values are presented. The skyplots of the GPS and the multi-GNSS constellation show the location of the satellites for the examined time interval. The high increase of the deviation of the GPS-only solution with respect to the multi-GNSS solution, due to the very low GPS satellite number, is reflected both in low- and high-frequency component

brings the availability to 73% and 80% for stations B and F, respectively (Figure 14), while the corresponding availability of a multi-GNSS solution is almost 100% for both stations. Even though the difference between VDOP of GPS-only and multi-GNSS satellite constellation might not be great (not more than 0.3), the quality of the signal of the limited GPS satellites is weak, leading to poor or even no GPS-only solution. The difference between the GPS-only and multi-GNSS solutions reaches or even exceeds the 50 mm, especially for the interval between 11:25 and 11:30 (Figure 14).

### 6.3 | Severn Bridge monitoring analysis: Points A and G

The analysis of points A and G confirmed the beneficial contribution of multi-GNSS for the time intervals which were revealed from the zero-baseline measurements and the other monitoring points. For instance, Figure 15 presents the lateral and vertical component time-series of Point A between 08:00 and 09:00, with the difference between the GPS-only and multi-GNSS solution in the low- and high-frequency band. The beneficial contribution of multi-GNSS solution is clear, as the GPS-only solution is characterised by poor satellite constellation due to the low number of GPS satellites (only four GPS satellites between 08:40 and 08:52), resulting to poor availability of GPS solution ( $\sim 43\%$ ), while the multi-GNSS solution has 100% availability and precision improvement exceeding 10 mm in both low- and high-frequency band.

Likewise, the GNSS data of point G were analysed and it was observed the beneficial contribution of the multi-GNSS for the periods of poor GPS satellite constellation and low availability of GPS solution, as for the other points (midspan and point A). Figure 16 presents the lateral and vertical component time-series of point G for the time interval between 11:00 and 12:00. For that period, it is observed that the multi-GNSS has higher availability than the GPS-

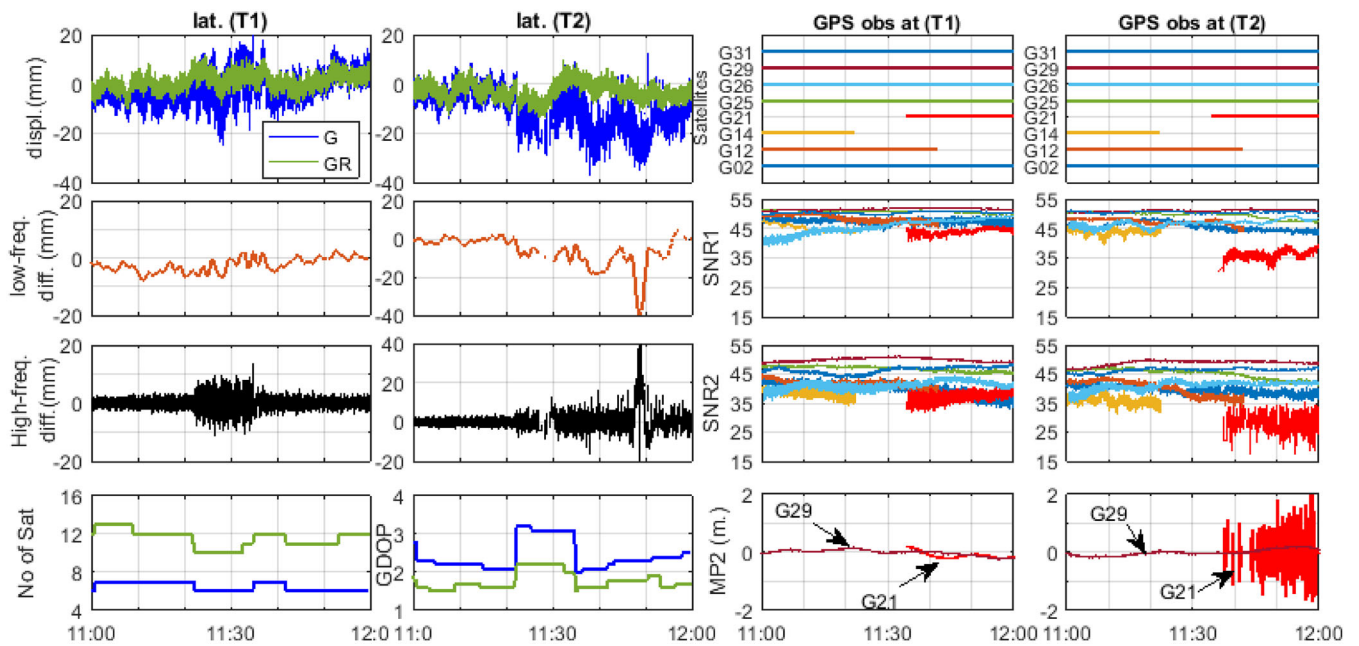


**FIGURE 10** The GPS-only and multi-GNSS displacement of the lateral displacement for T1 and T2 stations, with the differences of their corresponding low- and high-frequency components and the time series of the number of satellites and the corresponding GDOP values. Also the SNR and MP parameter time series are also presented for the GPS satellites, indicating the low-quality signal of the G21 satellite. The high deviation (peaks) of the GPS-only solution for the period 11:45–11:50 is strongly related to the high SNR and MP values for G21 satellite at T2 station

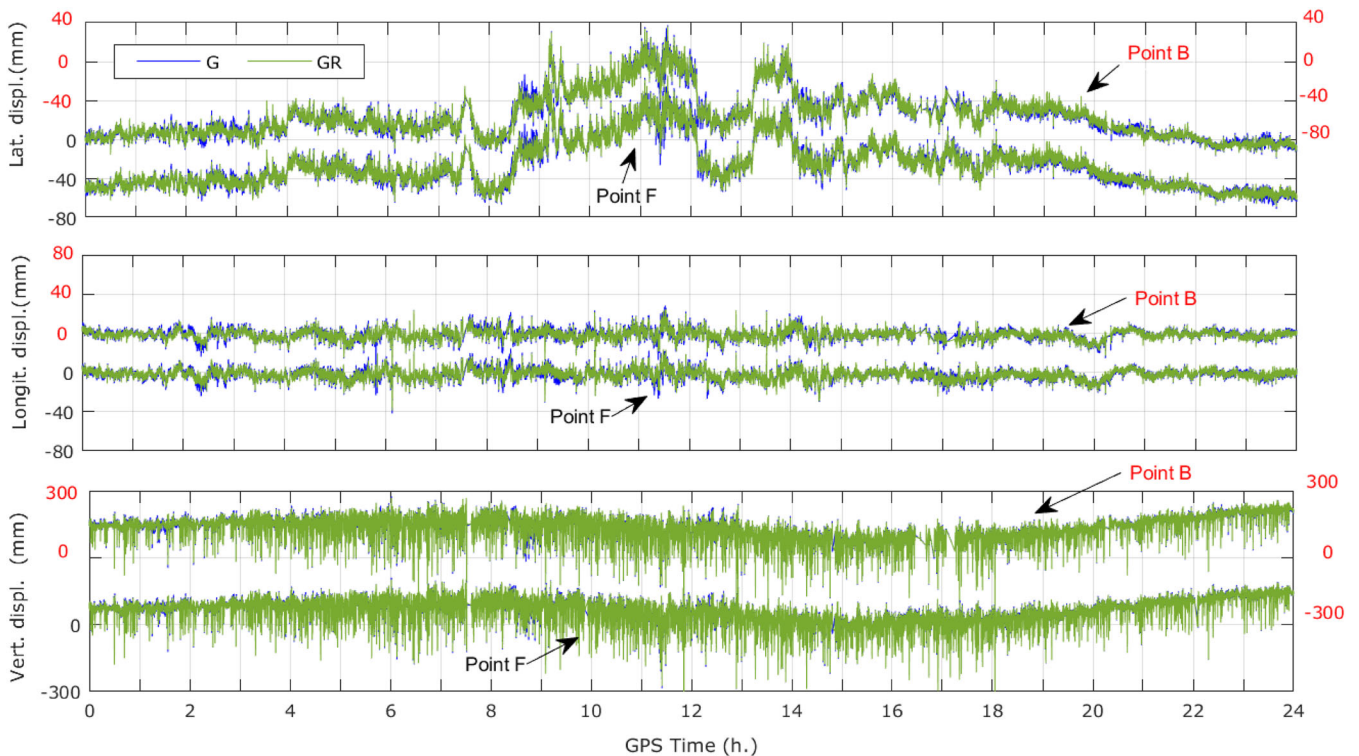


**FIGURE 11** Comparison of daily time series at cable stations B and F on the midspan of the bridge showing the comparison between components of displacements with GPS-only and multi-GNSS solutions on 22 July 2015. The GPS-only and multi-GNSS solutions seem to generally agree for the entire monitoring period

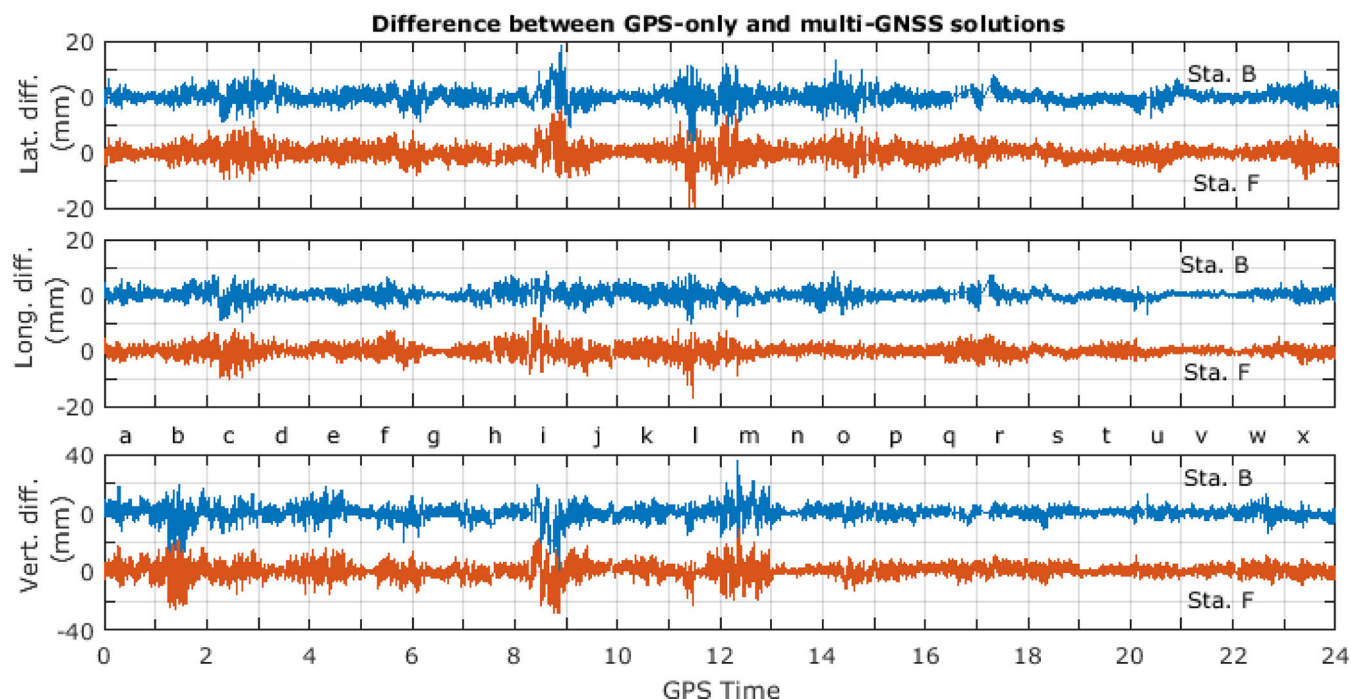


FIGURE 12 The time series of difference between GPS-only and multi-GNSS solutions for all the components of the midspan stations B and F that are presented in Figure 11. There are time intervals with consistent differences between GPS-only and multi-GNSS solution in lateral, longitudinal and vertical component, which are generally in agreement with the time intervals defined as GPS solution of low-precision from the zero-baseline measurements

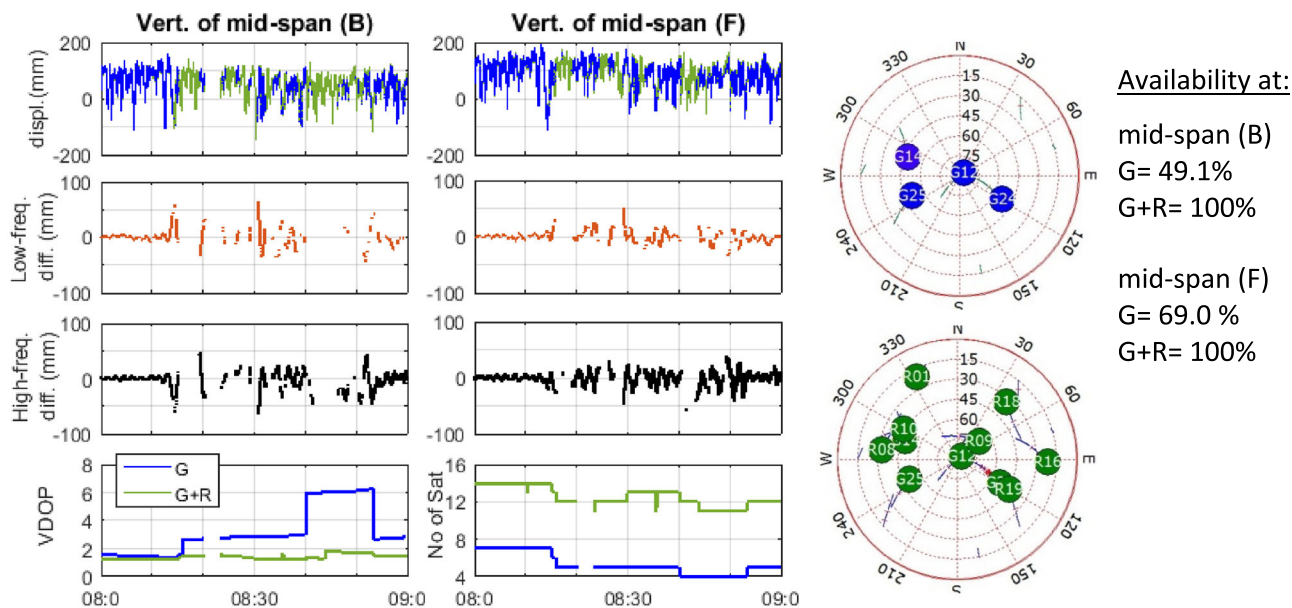
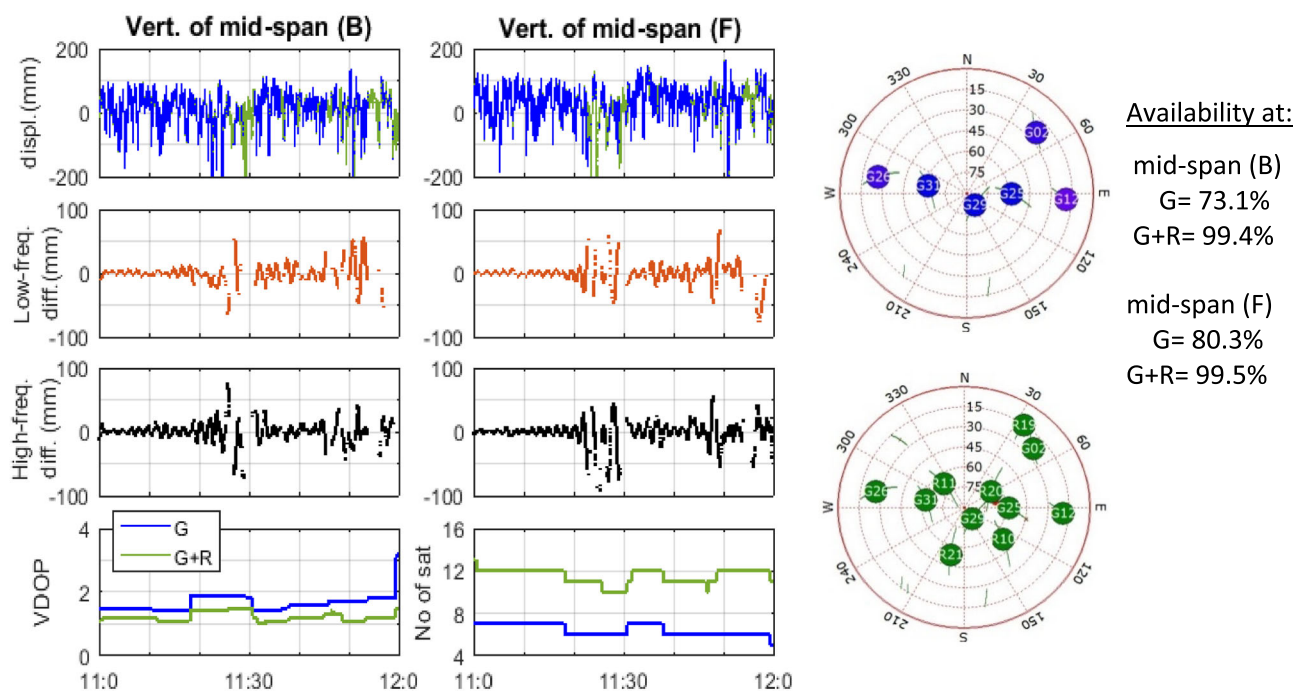


FIGURE 13 The GPS-only and multi-GNSS displacement of the vertical component for B and F with the differences of their corresponding low- and high-frequency components. The time series of the number of satellites for the GPS and multi-GNSS constellation and the corresponding VDOP values are presented. The skyplots of the GPS and the multi-GNSS constellation show the location of the satellites during the recording period. The poor GPS satellite constellation has an impact on the availability of the GPS-only solution as it is reduced even below 50% for point B



**FIGURE 14** The GPS-only and multi-GNSS displacement of the vertical component for B and F with the differences of their corresponding low- and high-frequency components. The time series of the number of satellites for the GPS and multi-GNSS constellation and the corresponding VDOP values are presented. The skyplots of the GPS and the multi-GNSS constellation show the location of the satellites during the recording period. The weak GPS constellation has a great impact on the availability of the GPS-only solution and the deviation from the multi-GNSS solution which reaches even up to 50–70 mm

only solution, reflected on the number of satellites and GDOP parameter. More specifically, it is observed the enhanced precision of the multi-GNSS which exceeds the 10 mm in low- and high-frequency component, mainly for the period of the low quality of GPS satellite constellation (i.e., 11:18–11:30). However, for the same time interval, the midspan points presented even lower availability of GPS-only solution (Figure 14), indicating the site-specific effects that may occur in the GNSS measurements, which can reduce the accuracy and the quality of the GPS-only solution, especially in an environment such that of a suspension bridge which is affected by obstructions and interference due to structural elements of the bridge.

## 6.4 | Severn Bridge monitoring analysis of 2010 GNSS data

From the GNSS 2010 monitoring campaign, only point C GNSS data was analysed, as at this point had a multi-GNSS receiver (Figure S1). By adopting the same methodology of the data analysis of 2015 GNSS campaign, the time intervals of poor GPS satellite constellation were detected, revealing periods where the number of GPS satellites dropped even to five satellites (Figure S2) and the addition of GLONASS satellites proved beneficial for the improvement of the availability and the accuracy of the multi-GNSS solution. Figure 17 presented the lateral and vertical component time-series of the GPS-only and multi-GNSS solution for the time-interval between 19:00 and 20:00, with the corresponding available satellites and DOP values. During that time interval, there is the period between 19:10 and 19:30 where the number of GPS satellites is low, varying between five and six satellites and resulting to poor satellite geometry, as it is reflected on the high GDOP values (i.e., GDOP ranging between 6 and 9.5). The addition of GLONASS satellites led to at least to eight available GPS and GLONASS satellites in total, improved the satellite geometry, as the GDOP value is reduced below 4 and resulted to the reduction of the noise level, which reached even 20 mm in low- and high-frequency components for the period of poor GPS satellite constellation. The beneficial contribution in other time intervals of point C of GNSS monitoring campaign of 2010 is presented in Figures S3 and S4.



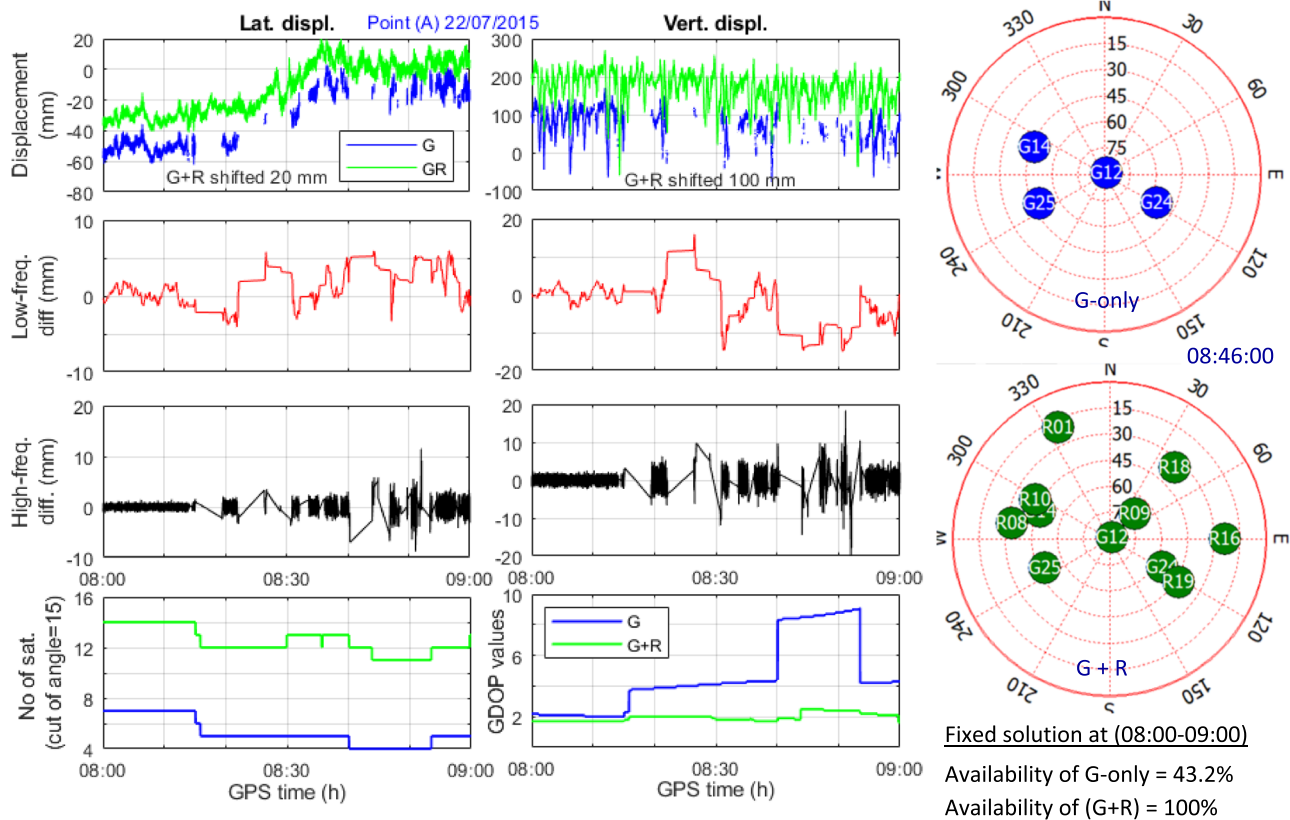


**FIGURE 15** The GPS-only and multi-GNSS displacement of the lateral and vertical component for A with the differences of their corresponding low- and high-frequency components. The time series of the number of satellites for the GPS and multi-GNSS constellation and the corresponding VDOP values are presented, showing the significant drop of the number of GPS satellites to five and then four satellites between 08:40 and 08:52. The skyplots of the GPS and the multi-GNSS constellation show the location of the satellites during the period with four visible GPS satellites. The weak GPS constellation has a significant impact on the availability of the GPS-only solution and the deviation from the multi-GNSS solution which reaches totally (in low- and high-frequency component) even up to 30–40 mm

## 6.5 | Severn Bridge response—Spectral analysis

For the estimation of the main modal frequencies of the bridge response, the GPS-only and multi-GNSS displacement time series of each component (lateral, longitudinal and vertical) were analysed by applying spectral analysis. For a reliable comparison between the modal frequencies derived by the GPS-only and multi-GNSS data spectral analysis, we focused only on the modal frequencies which fulfilled the following criteria: (i) to be confirmed from previous studies<sup>46,48</sup> of the response of Severn Suspension Bridge (Table 3), since the bridge design and/or bridge FEM model were not available, (ii) to derive from the analysis of time-intervals with low multi-GNSS noise and with conditions of bridge excitation/force dominant in one direction and (iii) to correspond to peaks of the spectra exceeding the 95% statistical significance. As most of the analysed time series are uncontinuous (with gaps), a suitable technique for spectral analysis is the Lomb Normalised Periodogram (LNP) using Norm-Period code, which also allows to define the statistical significance level of the spectra.<sup>2</sup> This method of estimating modal frequencies is known as peak picking (PP). There are more accurate and advanced methods (e.g., regression analysis and principal components<sup>56,57</sup>), but under conditions of low-damping and well-separated modal frequencies, the PP method is suffice. The case study of Severn Suspension Bridge can be considered as suitable for the PP method, since the bridge modal frequencies are considered as well-separated.<sup>56</sup> Furthermore, the assessment of the beneficial contribution of multi-GNSS was based on modal frequencies, which were confirmed by previous studies<sup>46,48</sup> and time intervals of known conditions of excitation/loading.

Due to the long records, the spectral analysis was applied at 10-min time periods, an approach which is broadly applied in bridge data analysis for the determination of the modal frequencies.<sup>1</sup> Firstly, the zero-baseline measurements were analysed, which are contaminated by errors due to the satellite constellation and the receiver noise, and the corresponding spectra should be characterised by white and potentially coloured noise.<sup>3</sup> This was confirmed by the

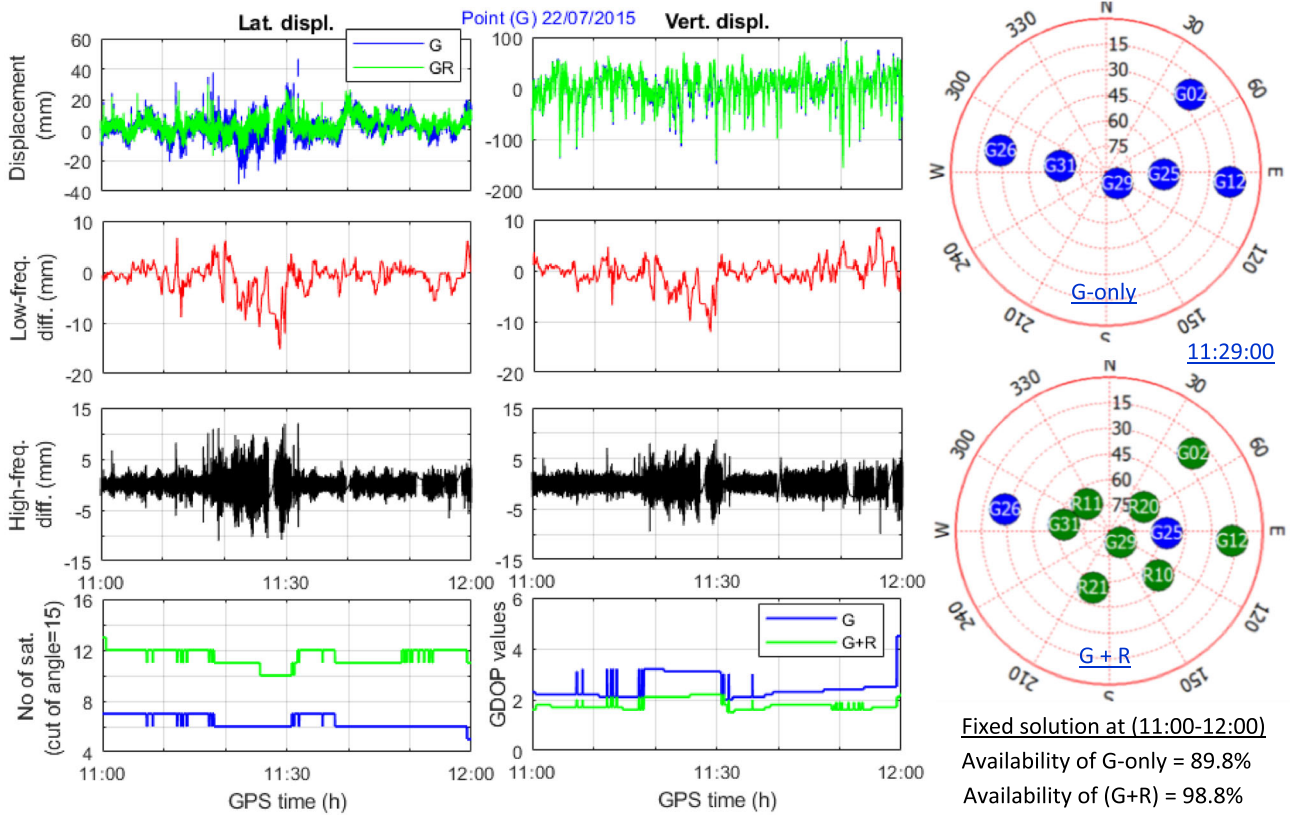


**FIGURE 16** The GPS-only and multi-GNSS displacement of the lateral and vertical component for G with the differences of their corresponding low- and high-frequency components. The time series of the number of satellites for the GPS and multi-GNSS constellation and the corresponding VDOP values are characterised by low number of GPS satellites and high GDOP value for the time interval between 11:18 and 11:30. The skyplots of the GPS and the multi-GNSS constellation show the location of the satellites for the period of the highest GDOP value. The weak GPS constellation has a great impact on the availability of the GPS-only solution and the deviation from the multi-GNSS solution which reaches totally up to 30 mm for the low- and high-frequency components

spectral analysis of the zero-baseline GPS-only and multi-GNSS coordinate time series, as there were no dominant frequencies detected, with the spectra expressing basically the noise level of the time series. Figure 18 shows the spectra of coordinate time series derived by the GPS-only and multi-GNSS solutions. It is evident that for the Easting component, where the GPS-only and multi-GNSS are of the same noise level, the corresponding spectra are identical. On the other hand for the Northing component, where the GPS-only solution has larger range of amplitude, the corresponding spectrum is characterised by higher noise but without any dominant peak.

The spectral analysis of the time series of the points T1, T2, B and F for the time interval 19:00–20:00 is used to identify the main modal frequencies of the midspan and the tower, as during that period, the GPS-only and multi-GNSS solutions are characterised by the lowest noise level during the 24-h interval, as it was also revealed from the zero-baseline measurements and the low GDOP values of GPS and multi-GNSS constellation for that interval. Figures 19 and 20 present the spectra of points B and T2. The peaks of those spectra, which exceed the 95% confidence level (which varies between 11.4 and 12.6 Hz depending on the displacement component), correspond to the frequencies of (i) 0.147 and 0.095 Hz in the vertical and lateral components at the midspan (point B), (ii) 0.158 Hz at the lateral and vertical components and (iii) 0.147 Hz in the longitudinal component at the tower (point T2). Those frequencies are also confirmed from the frequencies confirmed in previous studies.<sup>46,48</sup> The frequency of 0.147 Hz corresponds to the first vertical mode of the bridge and matches with the first modal frequency of the tower in the longitudinal axis. The frequency of 0.095 Hz corresponds to the first lateral mode of the bridge, which is typical for long-span bridges to be lower than the first vertical modal frequency (i.e., 0.147 Hz), and the frequency of 0.226 Hz which seems to correspond to the second vertical mode of the midspan.

To confirm the validity of these modal frequencies, we analysed periods where large traffic or wind load was applied. Figure 21 presents the multi-GNSS time series of point B at the midspan and point T2 at the tower. At the

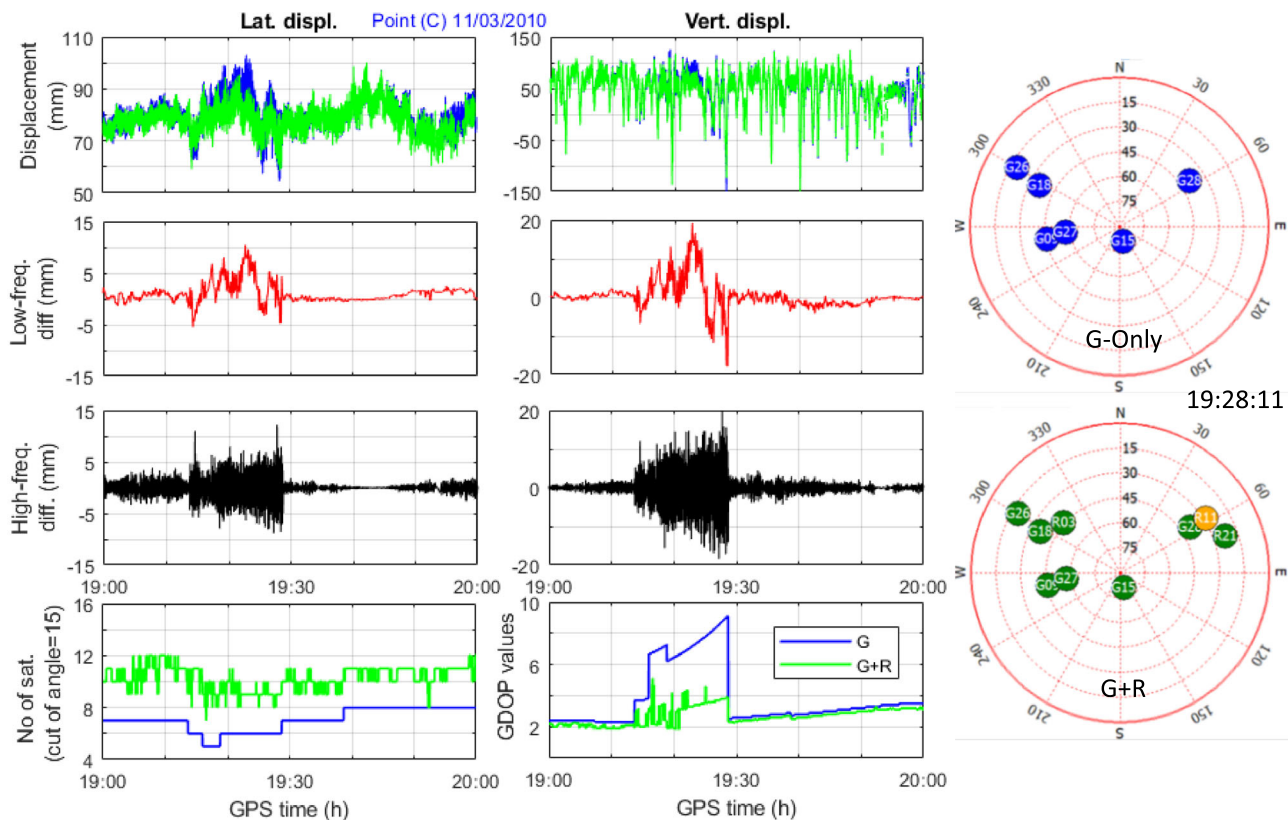


**FIGURE 17** The GPS-only and multi-GNSS displacement of the lateral and vertical component for point C with the differences of their corresponding low- and high-frequency components. The time series of the number of satellites for the GPS and multi-GNSS constellation and the corresponding VDOP values are presented, showing the period where the number of GPS satellites drops down to five and the GDOP varying between 6 and 9.5. The skyplots of the GPS and the multi-GNSS constellation show the location of the satellites for the period of the highest GDOP value. The weak GPS constellation has a significant impact on the availability of the GPS-only solution and the deviation from the multi-GNSS solution which reaches even up to 40 mm in total for the low- and high-frequency components

**TABLE 3** Modal frequencies of points B and F, which are used for the assessment of the beneficial contribution of multi-GNSS, indicating those who have been detected in previous studies of Severn Suspension Bridge

Mode	Estimated modal frequencies (in Hz)	Loading conditions	Modal frequencies from previous studies (in Hz)
1st lateral mode–midspan (Point B)	0.095	Wind load	Confirmed in Roberts et al. <sup>48</sup>
1st vertical mode–midspan (Point B)	0.147	Traffic load	Confirmed in Roberts et al. <sup>46,48</sup>
1st longitudinal mode–tower (Point T2)	0.147	Traffic load	Confirmed in Roberts et al. <sup>46</sup>
1st lateral mode–tower (Point T2)	0.158		Not confirmed
2nd vertical mode–midspan (Point B)	0.226	Traffic load	Confirmed in Roberts et al. <sup>46</sup>

displacement time series of the vertical component of point B, it is evident for the time interval between 19:02 and 19:04, a large vertical response reaching up to 150 mm, due probably to heavy vehicle(s) (i.e., lorries) crossing the bridge. This heavy load produces vibration at the midspan for the time interval between 19:04 and 19:05:30. This vibration is more evident after producing two high-pass filtered time series, with 0.1- and 0.2- cut-off frequencies, where a vibration-pattern response of increased amplitude is revealed for the time interval between 19:04 and 19:05:30.

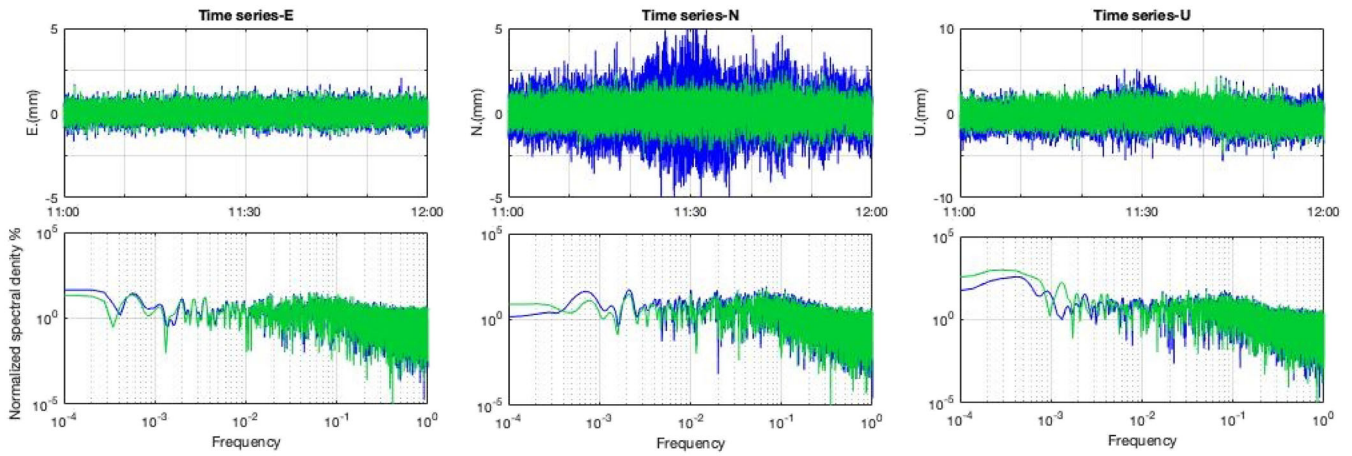


**FIGURE 18** (Top) The coordinate time series of E, N, U components of GPS-only and multi-GNSS solutions of the zero-baseline measurements. (Bottom) The spectra of the coordinate time series, where they all express noise, with no dominant frequency. It is evident the slightly higher noise level of GPS-only solution in the spectra mainly for the Northing component

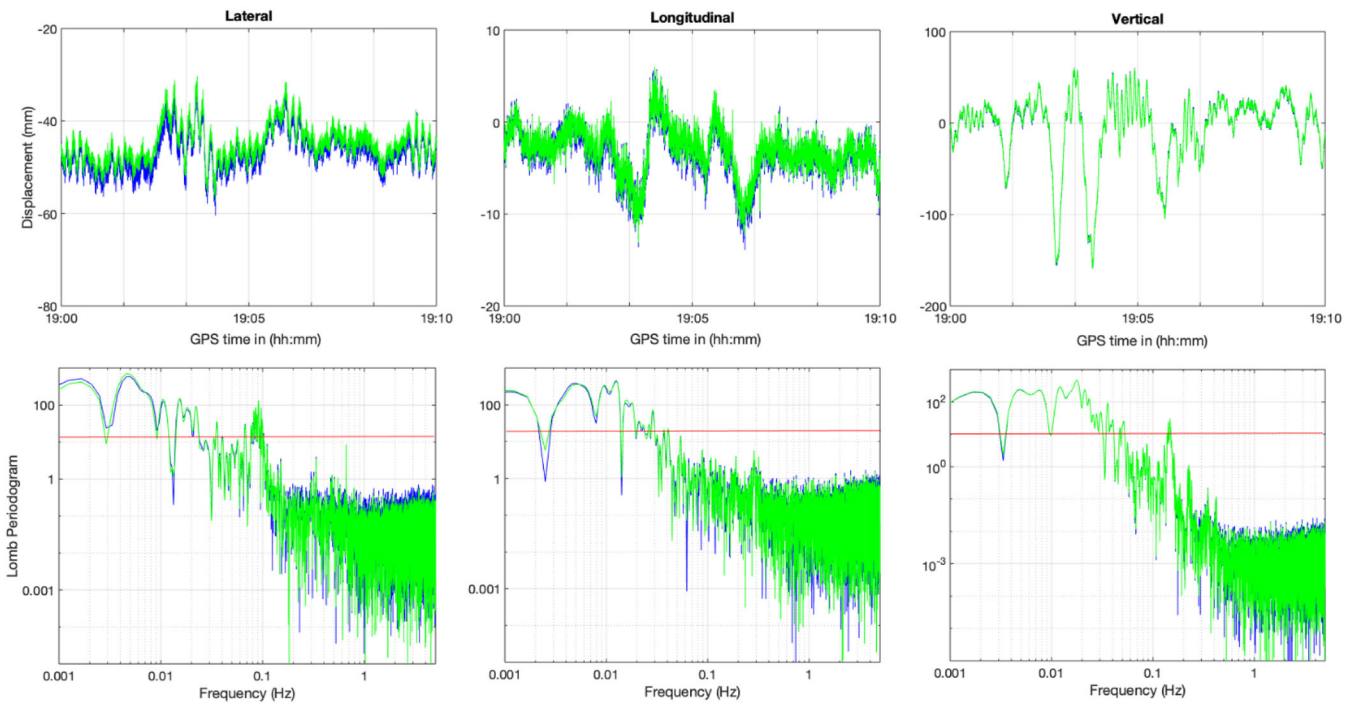


**FIGURE 19** (Top) Displacement time series of the lateral, longitudinal and vertical component of the GPS-only (blue) and multi-GNSS (green) solutions of point B for the time interval 19:00–19:10 of 22/07 and (bottom) the corresponding spectra, with the red line indicating the 95% confidence level. The main modal frequencies which are revealed from the spectral analysis are of 0.147 Hz in the vertical component and 0.095 Hz in the lateral component. The agreement between the GPS and multi-GNSS solution is also reflected in the spectra

Evidence of significant vibration is also observed in other periods of the filtered time series, which reflects the significance of modal frequencies of those frequency bands in the bridge response. Likewise, it was analysed the same time interval for the longitudinal multi-GNSS time series of the tower (point T2); a high-pass filter (0.1-Hz cut-off frequency) was applied, and the derived filtered time series is characterised by a vibration-pattern response which is dominant and with larger amplitude for the time interval between 19:04 and 19:05:30. The spectral analysis of the high-pass filtered (with 0.1-Hz cut-off frequency) time series led to spectra where the dominant frequencies are 0.147 and 0.226 Hz, for the midspan, and 0.147 Hz for the tower. The latter confirms that the modal frequency of 0.147 Hz is the first modal

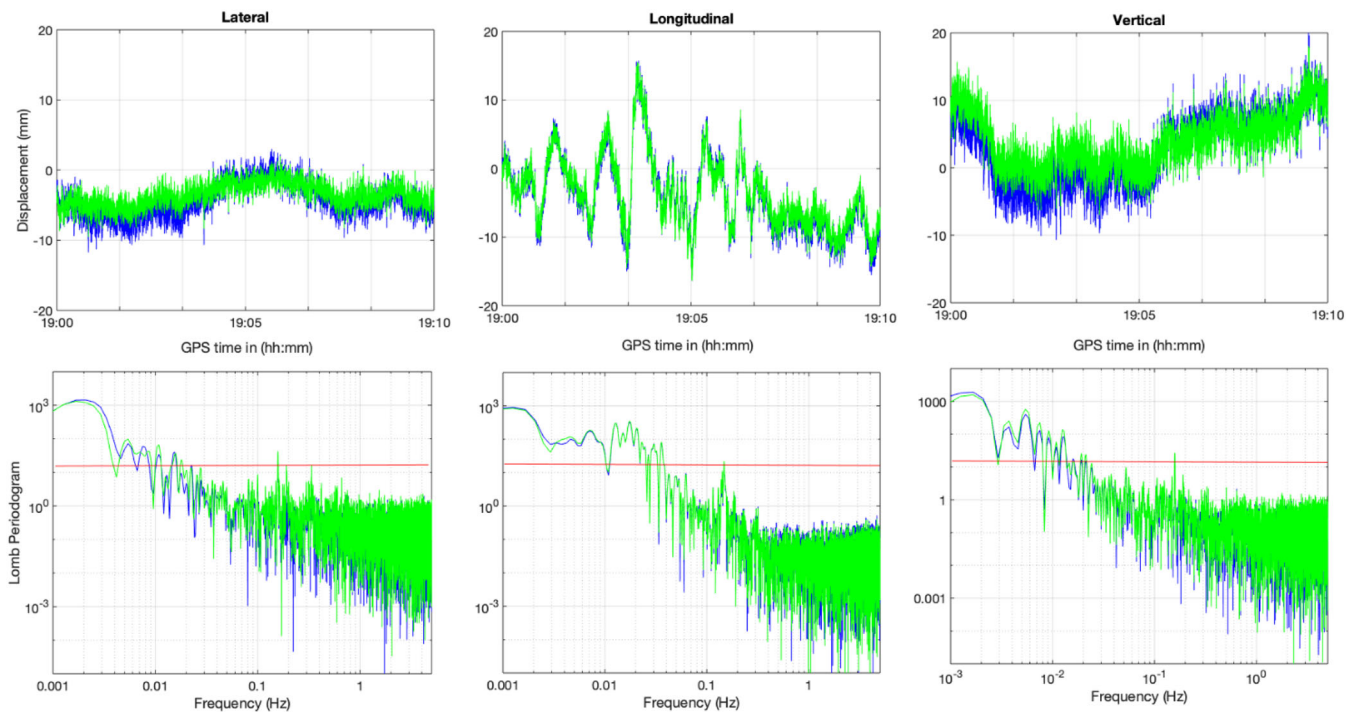


**FIGURE 20** (Top) Displacement time series of the lateral, longitudinal and vertical component of the GPS-only (blue) and the multi-GNSS (green) solutions of point T2 for the time interval 19:00–19:10 of 22 July and (bottom) the corresponding spectra, with the red line indicating the 95% confidence level. In the spectra are identified the modal frequencies of 0.147 Hz in the longitudinal component and 0.158 Hz in the vertical component, which exceed marginally the statistical significant level of 95%. The agreement between the GPS and multi-GNSS solution is also reflected in the spectra

frequency of the midspan, producing the main vibration at the midspan, which also produces the longitudinal response of the tower. The frequency of 0.226 Hz corresponds to vibration of smaller amplitude, and it is the second in order modal frequency of to the vertical component.

Regarding the modal frequency of 0.095 Hz, which corresponds to the lateral component of the midspan, we analysed the time interval between 12:00 and 12:10, where it was observed the strongest wind load, with the maximum wind speed occurring at 12:07 (wind speed  $\sim 40$  m/s; Figure 22). After applying a high-pass filter with 0.07-Hz cut-off frequency, the derived filtered time series is characterised by vibration-pattern response, with the larger amplitude occurring after 12:07, when the maximum wind lateral speed was observed. The spectral analysis of the high-pass filtered time series led to a spectra where the only dominant and statistically significant frequency is 0.095 Hz, indicating the first modal frequency corresponding to the lateral component.

To evaluate the beneficial impact of multi-GNSS time series, we focused in the time interval between 08:00 and 09:00, for which the GPS solution showed problems in availability due to the low number of satellites at point B, and there is significant difference between the spectra and the detected peaks of the GPS-only and multi-GNSS solutions. For instance, for the time interval of 08:10–08:20 and 08:30–08:40, where significant gaps are observed in the GPS solution, the spectra of the GPS solution are characterised by higher noise and the main modal frequencies of 0.147 (in the vertical component) and 0.095 Hz (in the lateral component) are not determined as clearly and precisely as in the multi-GNSS spectra (Figures 23 and 24). Furthermore, the frequency of 0.225 Hz in the vertical component, which can be detected in multi-GNSS spectrum, cannot be detected in the GPS spectrum due to the high noise level. It should be noted that for the time interval between 08:40 and 08:50, the modal frequencies could not be detected by the GPS spectrum due to the significant gaps in the corresponding time series (availability of GPS solution  $< 30\%$ ).

Likewise, for the point T2, the time interval between 22:30 and 22:40 is one with relatively poor GPS solution, as it is indicated by the GPS GDOP value which reaches even up to 5 and the difference between the GPS and multi-GNSS displacement time series (Figure 6). The spectral analysis of both GPS and multi-GNSS solutions reveals the main modal frequency of 0.147 Hz in the spectra of the longitudinal component, with that of multi-GNSS though being more

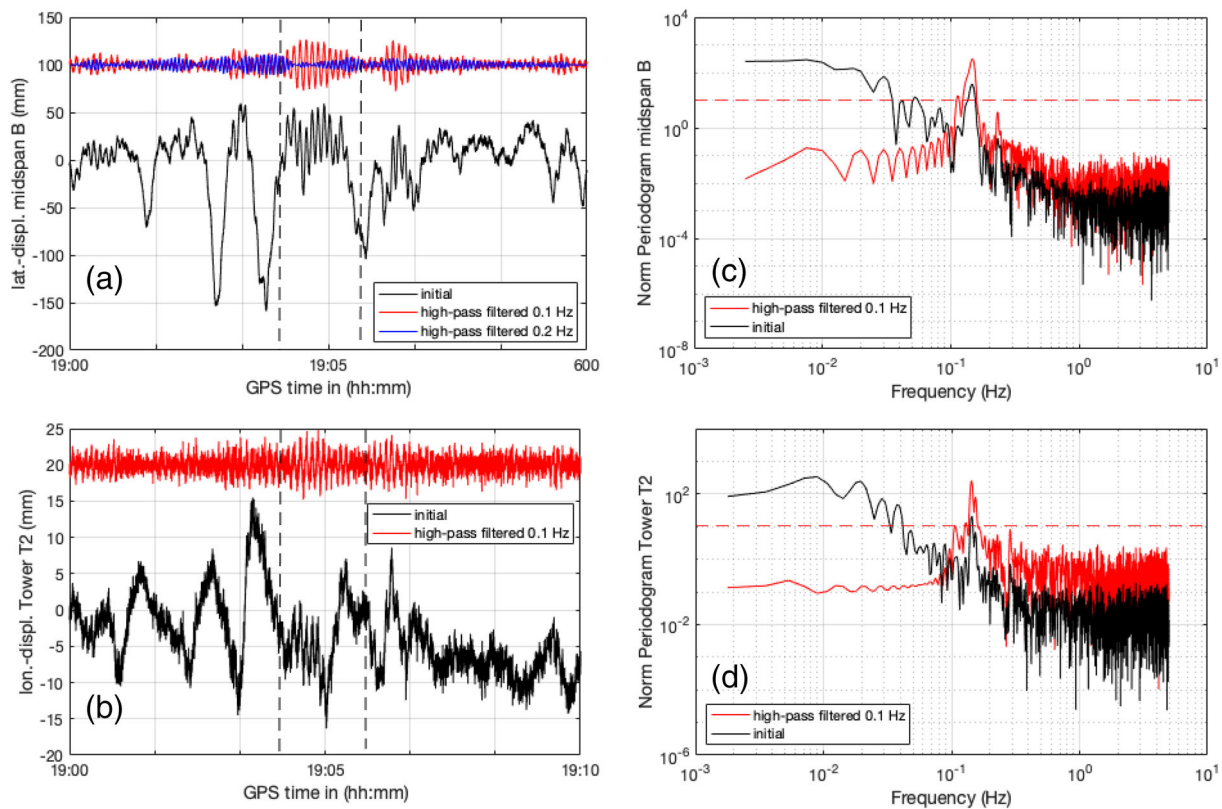


**FIGURE 21** Displacement multi-GNSS time-series of the (a) vertical component of the midspan-point B and (b) the longitudinal component of the tower-point T2 and the corresponding derived spectra (c,d). The dotted lines indicate the time-series interval (19:04–19:05:30) which follows the large midspan deflection of 150 mm. The high-pass filtered time series, which has an offset to be clearly separated in the plot from the initial time-series, has a larger vibration-type response for the time interval 19:04–19:05:30. In the spectra, the frequencies of 0.147 and 0.226 Hz are dominant in the vertical component of point B, and the frequency of 0.147 Hz is dominant in the longitudinal component of point T2

dominant as it corresponds to higher value in the periodogram (Figure 25). Furthermore, the frequency of 0.159 Hz is detected, as marginally statistically significant, in the spectra of the lateral and the vertical component, while they are not detected in the corresponding spectra of the GPS solution.

Hence, the main implication of a potential low precision or availability of GPS solution in the spectral analysis is the increased noise level in the corresponding spectrum, which may result to less clear identification of the frequencies peaks or even some frequencies may even be masked by the noise. In case of very low availability of GPS solution, it may even result to no detection of modal frequencies. In those cases, the multi-GNSS solution may lead to a more precise and clear spectrum leading to a more reliable detection of frequency peaks.

## 7 | DISCUSSION

The analysis of the GPS-only and multi-GNSS solutions for the response of Severn Bridge illustrates that their precision and accuracy depend strongly on the satellite system constellation which will be applied, especially for locations of unfavourable conditions (i.e., obstructions and strong multipath) which are met in bridge monitoring. It was shown that for time periods of weak GPS satellite constellation, as indicated by the corresponding GDOP value, to add an additional satellite system (e.g., GLONASS) will lead potentially to a more accurate GNSS solution, which can result to reliable estimation of the bridge response.

The main cases where the multi-GNSS solution led to a more reliable and precise estimation, with respect the GPS-only solution, were when:

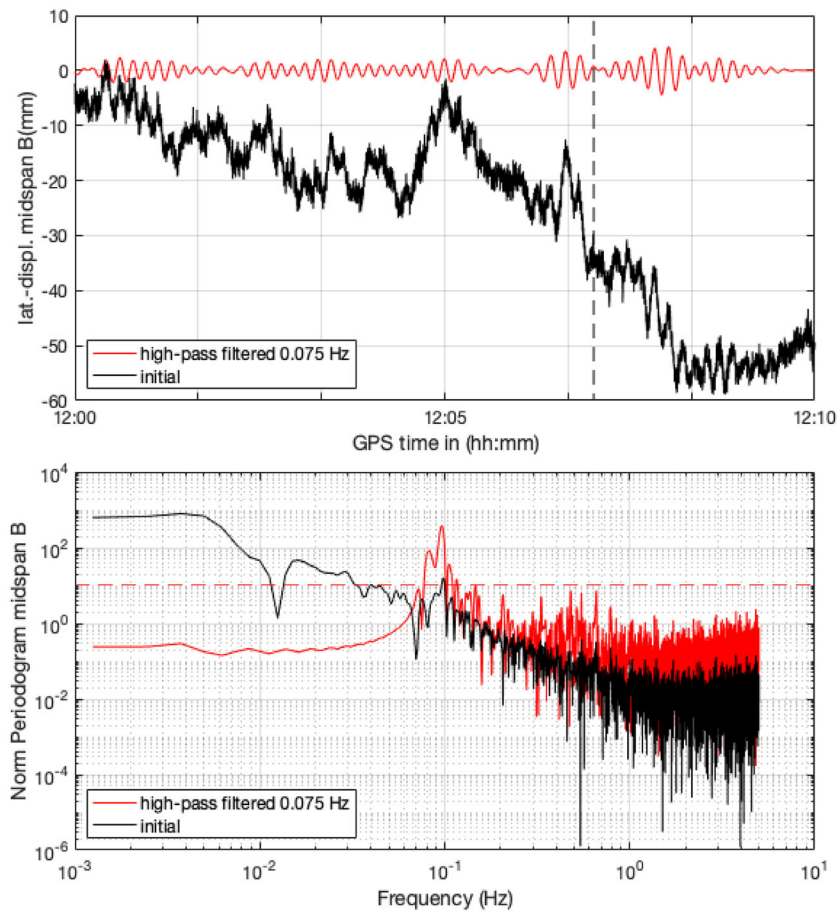


**FIGURE 22** (Top) Displacement multi-GNSS time series of the lateral component of the midspan point B and (bottom) the corresponding spectra. The high-pass filtered time series (red line) has the large vibration-type amplitude after 12:07 (indicated by the vertical dotted line), when the maximum lateral wind speed occurred. In the spectrum of the high-pass filtered, the frequency of 0.095 Hz is dominant corresponding to the main modal frequency in the lateral component of the midspan

- i. the number of the GPS satellites was low (in most of the cases  $\leq 5$  satellites) or the geometry of the GPS satellite constellation was weak ( $\text{GDOP} > 3$ ), which was also reflected on the zero-baseline measurements, and affected all the monitoring locations on the bridge (tower, midspan, etc.). In that case, the GPS-only solution had many data gaps which were resolved in the multi-GNSS solution.
- ii. site-specific effects due to the structure environment lead to obstruction and strong multipath, which again led to high noise level or even gaps in the solution. The site-specific effects were not detected in the zero-baseline measurements but were detected by the analysis of the satellites parameters (SNR, MP, etc.) for the each location. Again, the multi-GNSS solution led to much more precise solution, without the need even to exclude a satellite.

Furthermore, for both cases, there was impact in the estimation of the modal frequencies of the bridge, as the spectral analysis of the GPS-only solution led to more noisy spectra, where the noise level could mask the modal frequencies, or to less accurate spectra due to the gaps in the GPS-only solution.

However, the automatic application of multi-GNSS solution would not always lead to the most reliable solution, as satellite(s) from the other satellite constellation (for instance GLONASS) could malfunction result in higher noise level of the multi-GNSS solution.<sup>35</sup> Also, for solutions of GPS-only and multi-GNSS of the same accuracy and precision, the GPS-only should be preferred due to the shorter required computation time for the solution.

In the current study, the GNSS monitoring of the Severn Bridge was primarily designed in order to evaluate the impact of the different combinations of satellite constellation on the quality of the GNSS solutions and define the solution (GPS-only or multi-GNSS), which resulted in the most accurate estimation of the response and the modal frequencies of the bridge.

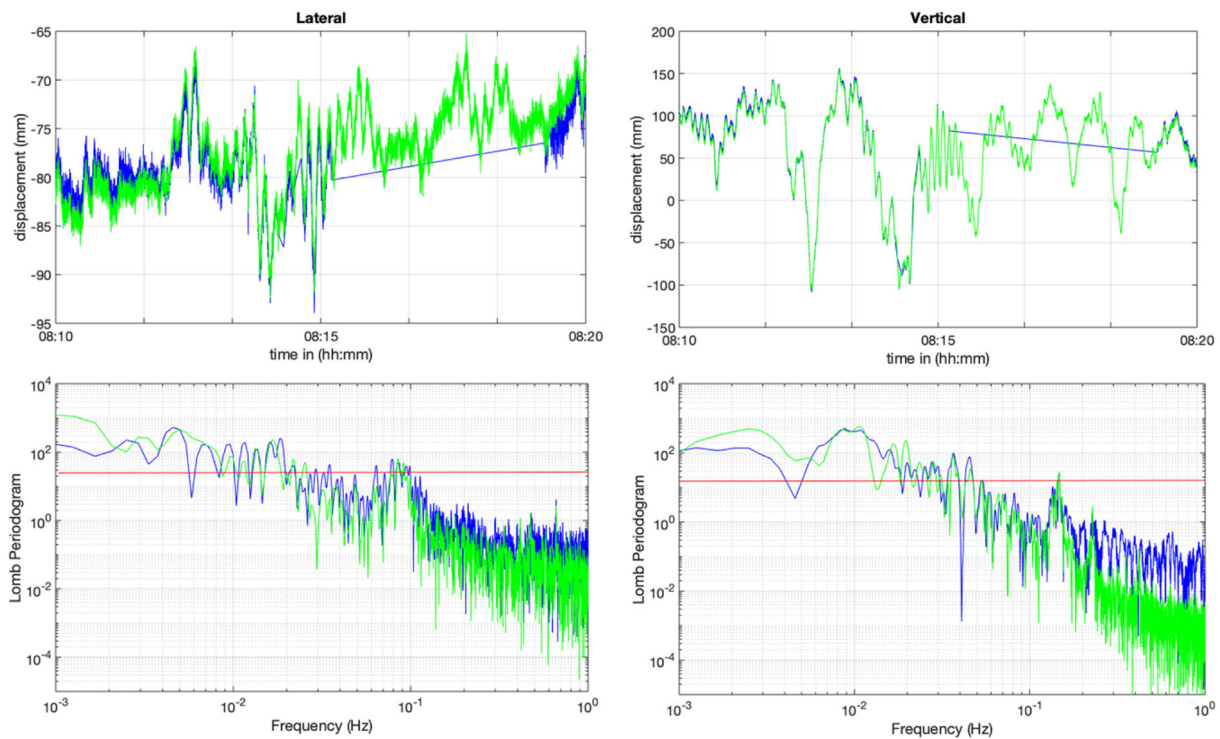


**FIGURE 23** (Top) Displacement time series of the lateral and vertical component of the GPS and multi-GNSS solution for the time interval between 08:10 and 08:20 of 22 July at point B. It is evident the 3-min data gap in the GPS solution. (Bottom) The spectra of the GPS and multi-GNSS time series, with the red line indicating the 95% confidence level. The GPS spectra are more noisy, which makes less clearly detected the main modal frequency of 0.095 Hz in the lateral component and the 0.225 Hz in the vertical component

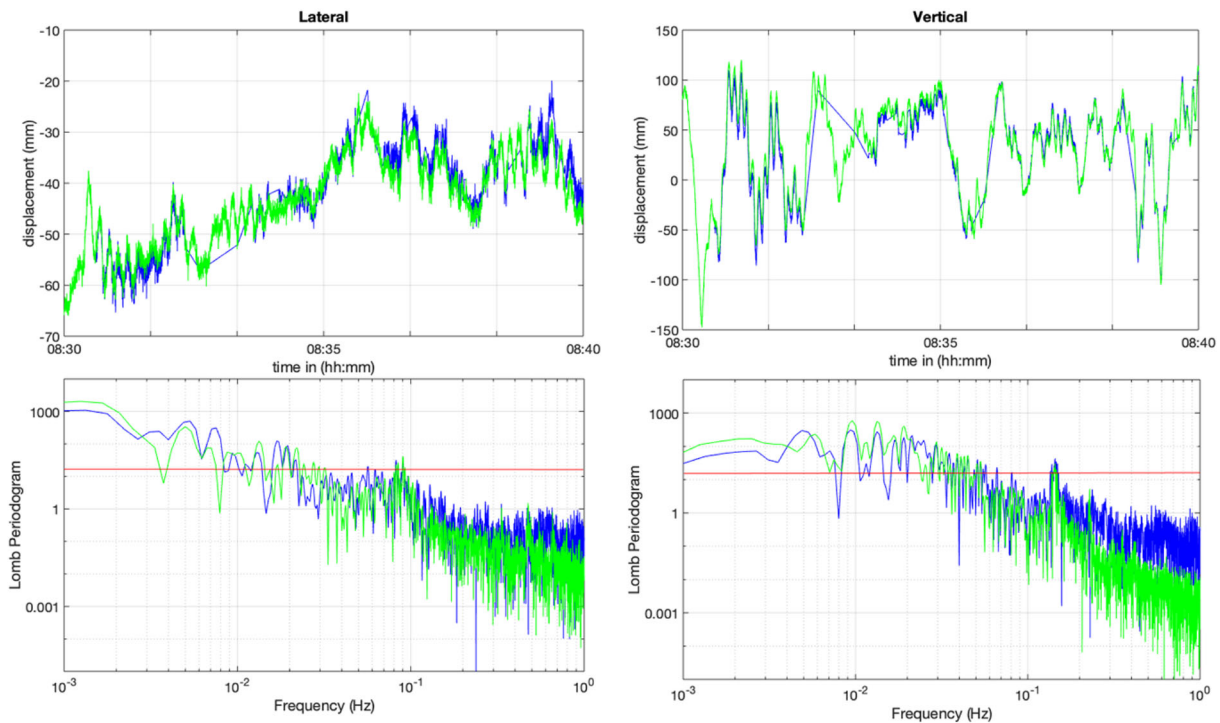


**FIGURE 24** (Top) Displacement time series of the lateral and vertical component of the GPS and multi-GNSS solution at the midspan point B, for the time interval between 08:30 and 08:40 of 22 July. It is evident the 3-min data gap in the GPS solution. (Bottom) The spectra of the GPS and multi-GNSS time series, with the red line indicating the 95% confidence level. Similar to Figure 18, the GPS spectra are more noisy, which makes less clear the detection of the main modal frequencies



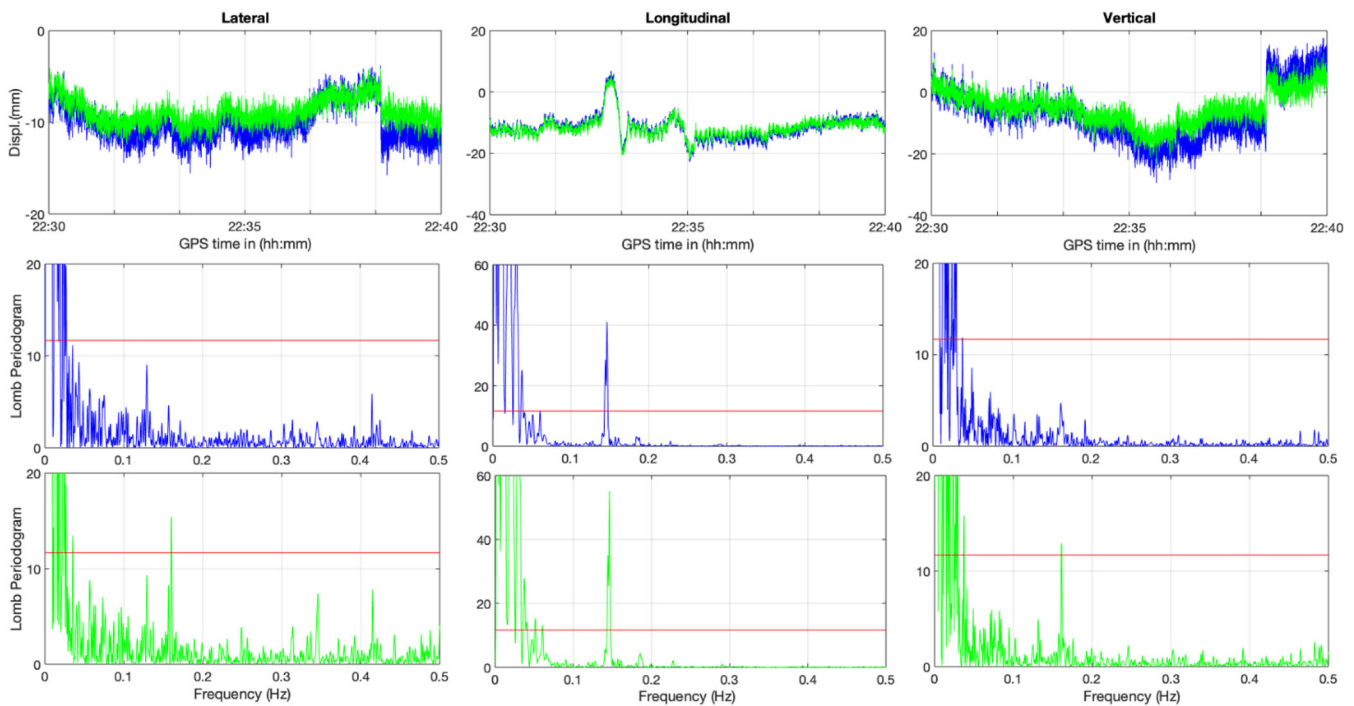


**FIGURE 25** (Top) Displacement time series of the lateral and vertical component of the GPS and multi-GNSS solution at the tower point T2, for the time interval between 22:30 and 22:40 of 22 July. The main modal frequency of 0.147 Hz is clearly detected in both GPS and multi-GNSS spectra, but for the multi-GNSS is statistically more significant. The modal frequency of 0.158 Hz is detected marginally in the lateral and vertical component spectra of the multi-GNSS solution

The methodology, which was applied for the analysis of the GPS-only and multi-GNSS solutions for the monitoring of Severn Bridge, can be applied for any health monitoring project of civil engineering structure. A main requirement is the zero-baseline measurements, which will be carried out at the reference station and used to evaluate the performance for each solution in every time period and indicate the optimum solution for the bridge response. However, further analysis of each station on the bridge needs to be made, as there are site-specific effects which may have impact on the individual station. More specifically, the steps of the developed methodology are the following (Figure 26):

- Step-1: Collection and cleansing of the GPS/GNSS records. The data of the bridge GNSS stations and the base stations (including the zero-baseline measurements) are collected and then cleaned. More specifically, based on the information deriving from the corresponding SNR, MP1 and MP2 parameters, the measurements corresponding to a specific satellite of low quality signal are identified and removed. If the signal of several satellites is of low quality for the specific epoch, then this epoch is removed from the processing.
- Step-2: Analyse the GDOP values of the available GNSS records. The GDOP values are estimated for all the available measurements and for every possible combination of satellite systems (GPS-only, GLONASS-only, multi-GNSS, etc.). Due to the short distances between the GNSS stations, their GDOP values should not deviate significantly. However, potential site-specific obstructions could produce deviations for specific GNSS stations, and the GDOP values are analysed for each GNSS station separately.
- Step-3: Processing of the GPS-only and multi-GNSS records. The GNSS base station and the GNSS bridge stations records are processed using DD mode. The main requirements of the configuration parameters are (i) to have  $15^\circ$  cut-off elevation angle for the satellites and (ii) to accept only the solution with fixed-ambiguity resolution. Solutions with no fixed ambiguities (i.e., float solution) are not further analysed. The same processing approach is used also for the zero-baseline measurements. This step results to the E,N,U time series for each GNSS combination for all the stations.
- Step-4: Conversion of E,N,U time series to bridge displacement time series. The NEU coordinate time series of each station are converted to the bridge coordinate system, by using the relative bridge position with respect the

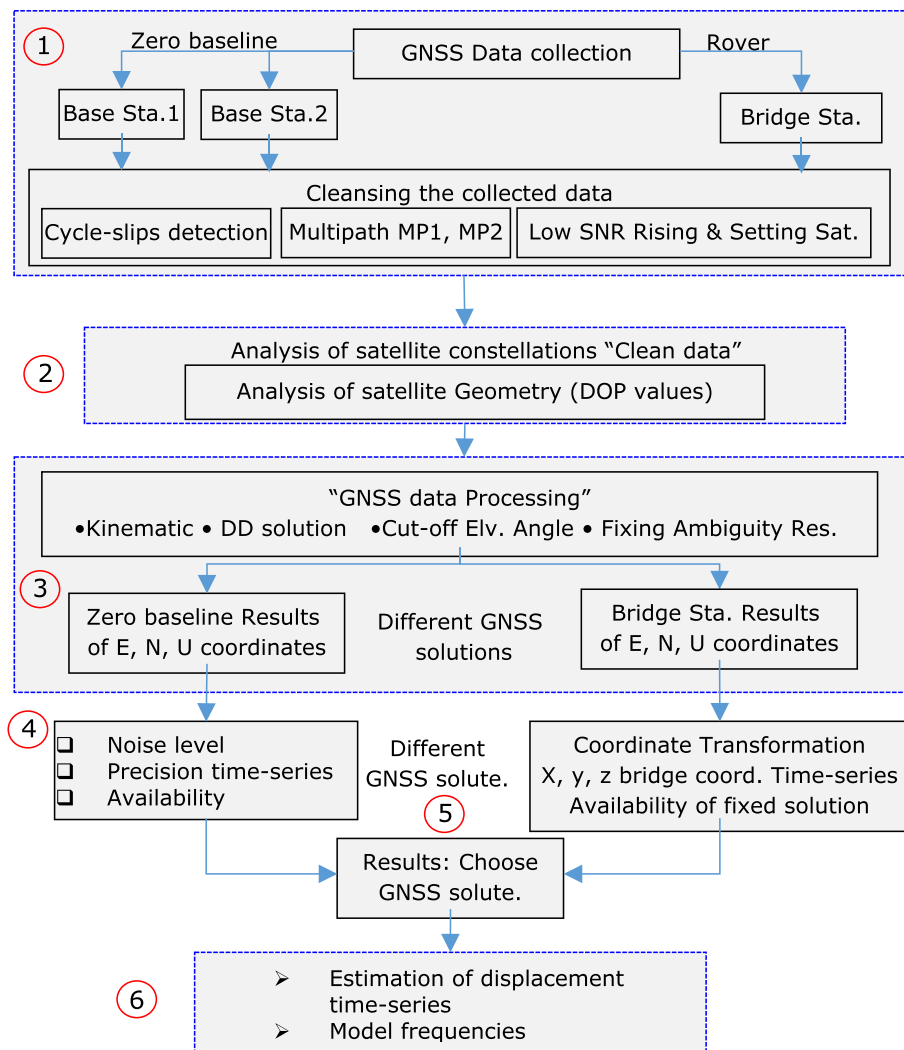


FIGURE 26 Flowchart representing the proposed monitoring methodology for Severn Suspension Bridge using multi-GNSS

GNSS coordinate and the transformation matrix. For the zero-baseline measurements, the NEU time series express the precision of the zero-baseline measurements.

Step-5: Based on the parameters of the geometry of the satellites (GDOP) and the indicators of satellite signal quality (SNR, MP), the quality of the GPS-only measurements and the multi-GNSS measurements is assessed for the bridge station and the zero-baseline station. The analysis of the zero-baseline NEU time series, considering the achieved precision and availability of the GPS-only and multi-GNSS solutions, should lead to the optimum GNSS solution. The former will be evaluated for every GNSS station on the bridge and can be altered for specific bridge GNSS station if there is an indication from the site-specific parameters of the GNSS measurements (GDOP, SNR, MP) for site-specific effects on GNSS measurements.

Step-6: The GNSS solution which is chosen from Step-5 is used to determine the displacement time series of the bridge and the estimation of the modal frequencies.

## 8 | CONCLUSIONS

The beneficial contribution of additional GNSS systems in enhancing the accuracy of GPS-only solution, thanks to the improved geometry of the multi-GNSS satellite constellation, is well-proved. However, the conditions under which the multi-GNSS solution is beneficial in bridge monitoring application, by improving the accuracy or the availability of

the bridge response estimation, was not further investigated. In this study, a new approach of multi-GNSS monitoring of the Severn Bridge was applied to investigate the impact of the multi-GNSS solution on the estimation of the response characteristics (amplitude and frequencies) of the bridge. The main hypothesis was that a multi-GNSS solution can overcome problems of the GPS-only solution, with respect the precision and the availability, due to satellite constellation weaknesses.

The GNSS monitoring of Severn Bridge showed that there are periods of weak geometry GPS constellation or poor quality (i.e., low SNR) of GPS satellite(s) signal, which could lead to noisy or even no solution and consequently the inaccurate estimation of the bridge response. For these periods, it was proved that an additional satellite system (GLONASS in this study) can lead to a significantly enhanced solution, more precise estimation of the displacement time series and clear detection of the main modal frequencies. Based on this study, a novel methodology is developed where the quality of the satellite system constellation (GPS-only and multi-GNSS) can be evaluated with zero-baseline measurements at the reference station and the measurements at each monitoring location. The analysis of these measurements determines which solution should be applied (GPS-only, multi-GNSS) to estimate the bridge response.

The outcome of this study is strongly affected by the location of the Severn Bridge and the corresponding quality of the GPS satellite constellation. For other geographical locations, the different geometry of the GPS satellite constellation will lead to different quality of GPS solutions. Furthermore, in this study, only the addition of GLONASS was examined due to the limited availability of Galileo and BeiDou at the time or the location of the recording, respectively. However, this methodology can be applied for the monitoring of any civil engineering structure, and it is expected that the addition of the satellite systems apart GPS will broaden the options of the multi-GNSS solutions, especially with the development of the low-cost multi-GNSS receivers,<sup>58</sup> and enhance the estimation of the structure response even further, especially for unfavourable monitoring locations and time periods of poor GPS solution.

## ACKNOWLEDGEMENTS

The manuscript was benefited by the comments of two anonymous reviewers. This work is partially supported by Ningbo Science and Technology Bureau under Commonweal Research Program with project code 2019C50017 and a research grant with project code A0060 from Ningbo Nottingham New Material Institute. The authors are very grateful to the Highways Agency and Severn River Crossing Plc for supporting and allowing the extensive field work to be carried out. The authors would like to thank the staff members on the Severn Bridge who were extremely helpful, particular in attaching the GNSS antennas to the structure.

## CONFLICT OF INTEREST

The authors declare that they have no conflicts of interest.

## AUTHOR CONTRIBUTIONS

Hussein Msaewe, Panos Psimoulis and Craig Hancock developed the strategy for data process and analysis. Hussein Msaewe processed the GPS data. Hussein Msaewe and Panos Psimoulis analysed the GNSS time series. Hussein Msaewe, Panos Psimoulis, Gethin Roberts and Lukasz Bonenberg carried out the field measurements. Hussein Msaewe and Panos Psimoulis wrote the paper, and Craig Hancock, Gethin Roberts and Lukasz Bonenberg proofread the paper.

## ORCID

Panos A. Psimoulis  <https://orcid.org/0000-0001-9013-4317>

## REFERENCES

1. Meng X, Nguyen D, Xie Y, et al. Design and implementation of a new system for large bridge monitoring—GeoSHM. *Sensors*. 2018; 18(3):775-798.
2. Psimoulis P, Pytharouli S, Karambalis D, Stiros S. Potential of Global Positioning System (GPS) to measure frequencies of oscillations of engineering structures. *J Sound Vib*. 2008;318(3):606-623.
3. Haberling S, Rothacher M, Zhang Y, Clinton JF, Geiger A. Assessment of high-rate GPS using a single-axis shake table. *J Geodesy*. 2015; 89(7):697-709.
4. Yi TH, Li HN, Gu M. Experimental assessment of high-rate GPS receivers for deformation monitoring of bridge. *Measurement*. 2013; 46(1):420-432.

5. Moschas F, Stiros S. Dynamic deflections of a stiff footbridge using 100-Hz GNSS and accelerometer data. *J Survey Eng.* 2015;141(4): 04015003.
6. Roberts GW, Dodson AH, Brown CJ, Karunar R, Evans A. Monitoring the height deflections of the Humber Bridge by GPS, GLONASS, and finite element modelling. In: *Geodesy Beyond 2000*. Springer; 2000:355-360.
7. Psimoulis PA, Stiros SC. Experimental assessment of the accuracy of GPS and RTS for the determination of the parameters of oscillation of major structures. *Comput Aided Civ Inf Eng.* 2008;23(5):389-403.
8. Moschas F, Stiros SC. Three-dimensional dynamic deflections and natural frequencies of a stiff footbridge based on measurements of collocated sensors. *Struct Control Health Monit.* 2014;21(1):23-42.
9. Moschas F, Stiros S. Measurement of the dynamic displacements and of the modal frequencies of a short-span pedestrian bridge using GPS and an accelerometer. *Eng Struct.* 2011;33(1):10-17.
10. Guo J, Xu L, Dai L, McDonald M, Wu J, Li Y. Application of the real-time kinematic global positioning system in bridge safety monitoring. *J Bridge Eng.* 2005;10(2):163-168.
11. Brown C, Roberts GW, Atkins C, Meng X, Colford B. Deflections and Frequency Responses of the Forth Road Bridge Measure by GPS. In: Lark R, ed. *Fifth International Conference on Current and Future Trends in Bridge Design, Construction and Maintenance*. Thomas Telford Publishing; 2007.
12. Koo KY, Brownjohn JM, List DI, Cole R. Structural health monitoring of the Tamar suspension bridge. *Struct Control Health Monit.* 2012;20(4):609-625.
13. Chen Q, Jiang W, Meng X, et al. Vertical deformation monitoring of the suspension bridge tower Using GNSS: A Case Study of the Forth Road Bridge in the UK. *Remote Sens (Basel).* 2018;10(3):364-383.
14. Yi T-H, Li HN, Gu M. Recent research and applications of GPS-based monitoring technology for high-rise structures. *Struct Control Health Monit.* 2012;20(5):649-670.
15. Su J, Su J, Xia W, Weng S. Review on field monitoring of high-rise structures. *Struct Control Health Monit.* 2020;27(12):e2629.
16. Breuer P, Chmielewski T, Górski P, Konopka E, Tarczyński L. Monitoring horizontal displacements in a vertical profile of a tall industrial chimney using Global Positioning System technology for detecting dynamic characteristics. *Struct Control Health Monit.* 2015;22(7): 1002-1023.
17. Yu J, Meng X, Shao X, Yan B, Yang L. Identification of dynamic displacements and modal frequencies of a medium-span suspension bridge using multimode GNSS processing. *Eng Struct.* 2014;81:432-443.
18. Wang J, Meng X, Qin C, Yi J. Vibration frequencies extraction of the forth road bridge using high sampling GPS data. *Shock Vibr.* 2016; 9807861.
19. Moschas F, Psimoulis PA, Stiros SC. GPS/RTS data fusion to overcome signal deficiencies in certain bridge dynamic monitoring projects. *Smart Struct Syst.* 2013;12(3-4):251-269.
20. Raziq N, Collier P. GPS deflection monitoring of the West Gate Bridge. *J Appl Geodesy Jag.* 2007;1(1):35-44.
21. Moschas F, Stiros S. Noise characteristics of high-frequency, short-duration GPS records from analysis of identical, collocated instruments. *Measurement.* 2013;46(4):1488-1506.
22. Roberts GW, Meng X, Dodson AH, Cosser E. Multipath mitigation for bridge deformation monitoring. *J Glob Position Syst.* 2002;1(1): 25-33.
23. Han HZ, Wang J, Meng X, Liu H. Analysis of the dynamic response of a long span bridge using GPS/accelerometer/anemometer under typhoon loading. *Eng Struct.* 2016;122:238-250.
24. Psimoulis PA, Stiros SC. A supervised learning computer-based algorithm to derive the amplitude of oscillations of structures using noisy GPS and Robotic Theodolites (RTS) records. *Comput Struct.* 2012;92-93:337-348.
25. Montillet J-P et al. Deploying a Locata network to enable precise positioning in urban canyons. *J Geodesy.* 2009;83(2):91-103.
26. Bonenberg L, Roberts G, Hancock C. Using Locata to augment GNSS in a kinematic urban environment. *Arch Ph Cart Rem Sens.* 2011; 22:63-74.
27. Psimoulis P, Houlié N, Meindl M, Rothacher M. Consistency of PPP GPS and strong-motion records: case study of Mw9.0 Tohoku-Oki 2011 earthquake. *Smart Struct Syst.* 2015;16(2):347-366.
28. Stiros S, Psimoulis P, Kokkinou E. Errors introduced by fluctuations in the sampling rate of automatically recording instruments: experimental and theoretical approach. *J Survey Eng Asce.* 2008;134(3):89-93.
29. Truong DM, Ta TH. Development of real multi-GNSS positioning solutions and performance analyses. in *Advanced Technologies for Communications (ATC), 2013 International Conference on.* 2013. IEEE
30. Yu XD, Gao JX. Kinematic precise point positioning using multi-constellation Global Navigation Satellite System (GNSS) observations. *ISPRS Int J Geo Inf.* 2017;6(1):6.
31. Abd Rabbou M, El-Shazly A, Ahmed K. Comparative analysis of multi-constellation GNSS single-frequency precise point positioning. *Survey Rev.* 2017;1-10.
32. Cai CS, Gao Y. Modeling and assessment of combined GPS/GLONASS precise point positioning. *Gps Sol.* 2013;17(2):223-236.
33. Li X, Zhang X, Ren X, Fritsche M, Wickert J, Schuh H. Precise positioning with current multi-constellation Global Navigation Satellite Systems: GPS, GLONASS, Galileo and BeiDou. *Sci Rep.* 2015;5:8328.
34. Cai CS, Gao Y, Pan L, Zhu J. Precise point positioning with quad-constellations: GPS, BeiDou, GLONASS and Galileo. *Adv Space Res.* 2015;56(1):133-143.

35. Msaewe HA, Hancock CM, Psimoulis PA, Roberts GW, Bonenberg L, de Ligt H. Investigating multi-GNSS performance in the UK and China based on a zero-baseline measurement approach. *Measurement*. 2017;102:186-199.
36. Lepadatu A, Tiberius C. GPS for structural health monitoring—case study on the Basarab overpass cable-stayed bridge. *J Appl Geodesy*. 2014;8(1):65-86.
37. de Bakker PF, Tiberius CCJM, van der Marel H, van Bree R. Short and zero baseline analysis of GPS L1 C/A, L5Q, GIOVE E1B, and E5aQ signals. *GPS Sol*. 2012;16(1):53-64.
38. Drózdź M, Szpunar R. GNSS receiver zero baseline test using GPS signal generator. *Artif Sat*. 2012;47(1):13-22.
39. Hofmann-Wellenhof B, Lichtenegger H, Wasle E. GNSS—global navigation satellite systems: GPS, GLONASS, Galileo, and more. 2007: Springer Science & Business Media.
40. Subirana JS, Zornoza JJ, Hernández-Pajares M. GNSS Data processing. Volume 1: fundamentals and algorithms. ESA Communications ESTEC, PO Box, 2013. 299: p. 2200.
41. Peppas I, Psimoulis P, Meng X. Using the signal-to-noise ratio of GPS records to detect motion of structures. *Struct Control Health Monit*. 2018;25(2):e2080.
42. Amiri-Simkooei A, Tiberius C. Assessing receiver noise using GPS short baseline time series. *GPS Sol*. 2007;11(1):21-35.
43. Deng C, Tang W, Liu J, Shi C. Reliable single-epoch ambiguity resolution for short baselines using combined GPS/BeiDou system. *GPS Sol*. 2014;18(3):375-386.
44. Dong D, Wang M, Chen W, et al. Mitigation of multipath effect in GNSS short baseline positioning by the multipath hemispherical map. *J Geodesy*. 2016;90(3):255-262.
45. Roberts GW, Brown CJ, Tang X, Meng X, Ogundipe O. A tale of five bridges; the use of GNSS for monitoring the deflections of bridges. *J Appl Geodesy*. 2014;8(4):241-264.
46. Roberts GW, Brown CJ, Tang X, Ogundipe O. Using satellites to monitor Severn Bridge structure, UK. *Proc Inst Civil Eng Bridge Eng*. 2015;168(4):330-339.
47. Msaewe H, Hancock C, Psimoulis P, Roberts GW, Bonenberg L. Monitoring Dynamic Deflections at Towers of Severn Suspension Bridge in the UK Using GNSS Technique. Proceedings of the ISGNSS, Hong Kong, China, 2017: pp. 10-13.
48. Roberts G, Tang X, Brown CJ. Measurement and correlation of displacements on the Severn Suspension Bridge using GPS. *J Appl Geomat*. 2019;11(2):161-176.
49. Moschas F, Stiros S. Dynamic multipath in structural bridge monitoring: An experimental approach. *GPS Sol*. 2014;18(2):209-218.
50. Al-Shaery A, Zhang S, Rizos C. An enhanced calibration method of GLONASS inter-channel bias for GNSS RTK. *Gps Sol*. 2013;17(2): 165-173.
51. Takasu T. RTKLIB ver. 2.4. 2 manual, RTKLIB: an open source program package for GNSS positioning. Tokyo University of Marine Science and Technology, Tokyo, 2013.
52. Dach R, Hugentobler U, Fridez P, Meindl M. Bernese GPS Software Version 5.0. Astronomical Institute, University of Bern. Berne, Switzerland, 2007.
53. Breuer P, Chmielewski T, Górski P, Konopka E. Application of GPS technology to measurements of displacements of high-rise structures due to weak winds. *J Wind Eng Industr Aerodyn*. 2002;90(3):223-230.
54. Cosser E, Roberts GW, Meng X, Dodson AH. The comparison of single frequency and dual frequency GPS for bridge deflection and vibration monitoring. in Proc of the Deformation Measurements and Analysis, 11th International Symposium on Deformation Measurements, International Federation of Surveyors (FIG). 2003.
55. Tokura H, Yamada H, Kubo N, Pullen S. Using multiple GNSS constellations with strict quality constraints for more accurate positioning in urban environments. *Positioning*. 2014;5(04):85-96.
56. Peeters B, de Roeck G. Stochastic system identification for operational modal analysis: A review. *Journal of Dynamic Systems. Measure Control*. 2001;123(4):659-667.
57. Magalhaes F, Cunha A, Caetano E. Vibration based structural health monitoring of an arch bridge: From automated OMA to damage detection. *Mech Syst Signal Process*. 2012;28:212-228.
58. Xue C, Psimoulis P, Zhang Q, Meng X. Analysis of the performance of closely spaced low-cost multi-GNSS receivers. *Applied Geomatics*. 2021. <https://doi.org/10.1007/s12518-021-00361-8>

## SUPPORTING INFORMATION

Additional supporting information may be found in the online version of the article at the publisher's website.

**How to cite this article:** Msaewe HA, Psimoulis PA, Hancock CM, Roberts GW, Bonenberg L. Monitoring the response of Severn Suspension Bridge in the United Kingdom using multi-GNSS measurements. *Struct Control Health Monit*. 2021;e2830. doi:10.1002/stc.2830